

Onno Bokhove

Maths fights floods

–managing river floods in an age of extremes

November 25, 2023

Springer Nature

“J’ai de sérieuses raisons de croire que la planète d’où venait le petit prince est l’astéroïde B 612. Cet astéroïde n’a été aperçu qu’une fois au télescope, en 1909, par un astronome turc.

Il avait fait alors une grande démonstration de sa découverte à un congrès international d’astronomie. Mais personne ne l’avait cru à cause de son costume. Les grandes personnes sont comme ça.

Heureusement pour la réputation de l’astéroïde B 612, un dictateur turc imposa à son peuple, sous peine de mort, de s’habiller à l’européenne. L’astronome refit sa démonstration en 1920, dans un habit très élégant. Et cette fois-ci tout le monde fut de sons avis.”

—Le Petit Prince, Antoine de Saint-Exupéry. Édition Gallimard 1999.

Foreword

First, the 2015 Boxing Day floods in Leeds form the starting point to address how we can explain the magnitudes of extreme river floods to the general public and how we can communicate/improve flood-mitigation plans and the decision-shaping process? Furthermore, what constitutes good flood-mitigation and how can we take good decisions? These questions gained importance due to climate change and the increased risk of severe flooding. Second, the Wetropolis flood demonstrator was designed based on mathematical modeling. It showcases return periods and uncertainty classifying extreme rainfall/flooding events in a portable set-up. An easy-to-understand description of Wetropolis is developed as well as mathematical models. Meant originally for the public, Wetropolis triggers and has triggered development of a graphical science-policy cost-effectiveness tool of flood-mitigation plans. This graphical tool is deliberately straightforward with minimal mathematics as used by municipalities in the EU. Building blocks of the tool are introduced step-by-step, using data of global river floods, for both interested mathematicians and the general public. Finally, . . . [decision-making].

Preface

The title “*Maths fights floods*” was the title of a failed EPSRC program grant submitted by the author with the management board and a participant of the UK “Maths Foresees” EPSRC Living with Environmental Change network. We did reach the interview stage. It is also the title of a Study Group Mathematics with Industry report of the 2008 Study Group held at the University of Twente, The Netherlands, co-organised and led by the author. In both instances, these were work titles which never changed. The subtitle was in essence the title given to the author by Robin Gray (Pennine Prospects) for a presentation at the 2016 workshop on flooding for the general public in Hebden Bridge, UK, organised after the devastating 2015 Boxing Day floods.

Chapter 1: The owner Mike Rawlinson of the Xfit The Forge Gym took the photograph in Fig. 1.3 of the floodwaters caused by Storm Ciara. The coastal wave tank images from JBA Trust and Thomas Goodfellow in Fig. 1.4 have been used with their permission. Dukan Borman and the author had supervised the coastal-wave-tank MSc project in 2015. The Wetropolis flood demonstrator plan of Fig. 1.5 was made by the author.

Chapter 2: First analyses of three sets of river-flood data were undertaken in student projects (2018–2021) by Antonia Feilden (River Ouse, UK), Zheming Zhang (River Don, UK) and Nico Septianus (River Ciliwung, Indonesia [44]) with improvements to the latter River Ciliwung analysis by Shunyu Yao and Yantong Ge. Shunyu Yao also initiated and made the Yangtze River analysis at Cuntan, China, which flood-excess volume has been used in Table 2.2. The *Python* codes of Mary Saunders, Antonia Feilden and Zheming Zhang, each concerning one specific river flood, formed the basis of my single code *rivertestgentest.py*, which has been used to (re)plot various river floods displayed in this Springer brief. Codes are available on the GitHub page <https://github.com/Flood-Excess-Volume/RiverDon>. It is a pleasure to acknowledge the visit to the Wainfleet Flood Action Group (WFAG) on 19-08-2019. It was hosted by local expert Stewart Peltell who explained and showed various hydraulic features around Wainfleet to the author. Circa 200m from the repaired breach seen in Fig 2.5, a weak spot was found in the berm at the venturi channel of the relief canal underneath the railway, which we promptly reported to

the Environment Agency –who had noticed the weak spot but had neither communicated the weak spot to WFAG nor repaired it alongside the repair of the breach. On 12-03-2020, just before the lockdown for the Covid-19 pandemic, the author went on marvellous tour to a beaver colony in North Yorkshire with fellow Bradford citizen and chair of the Aire Rivers Trust Geoff Roberts, a tour kindly organised by ecologist Cath Bashford of the Yorkshire Forest district. A few photograph and ideas unfolded in this brief arose during that tour.

Chapter 3: The basic schematic of Fig. 3.1 was made by Wout Zweers with some assistance, based on a simplification of such a schematic made by Jean-Marc Tacnet, the latter one as used in [9]. The two river-flood cases considered in Chapter 3 are based on work by Bokhove et al. [1] and Piton et al. [39] (Part 5). Data for a revisited analysis of the River Glinščica, Slovenia, were kindly provided by Alessandro Pagano and Polona Pengal; basic river-flood data were replotted in *Python* extended with an error analysis by the author. The analysis on the River Don was archived as a report in [1] (not peer-reviewed) and has largely been taken over with minor modifications as well as with permission of use by co-authors Mark Kelmanson and Tom Kent.

Chapter 4: This chapter on the Wetropolis flood demonstrator is largely based on rewriting published work in [8, 5] and joint work in progress [22, 23], for which collaborator co-author Tom Kent has given permission.

Comments and suggestions by Guillaume Piton led to various improvements throughout this brief. Wout Zweers kindly contributed in various ways.

The author acknowledges the Environment Agency for kindly providing data of various, but in particular the Armley, Skelton, Mytholmroyd Gunnislake and Sheffield Hadfields, UK river gauges and rating curves for these sites. As such this brief has used public-sector information licensed under the Open Government Licence v3.0.

June–October 2021

Apperley Bridge, UK and Joure, Friesland,
Onno Bokhove

Contents

1	Introduction	1
1.1	Questions on flooding: background and history	1
1.2	How do we explain return periods to the general public?	7
1.3	How do we communicate flood-mitigation plans?	12
1.4	Outline	15
2	How do humans and beavers view river floods?	17
2.1	Introduction	17
2.2	River-level measurements	19
2.3	The role of rating curves	21
2.4	Hydrographs and flood-excess volume	24
2.5	Storage-based protection measures	27
2.6	Available flood-storage volume	30
2.7	Upscaling flood-water storage behind beaver dams unrealistic?	32
2.8	Controlling water levels: human versus beaver engineering	38
3	On communicating flood-mitigation plans	43
3.1	Introduction and history	43
3.2	Visualisation of river data revisited	46
3.2.1	River Glinščica, Slovenia	46
3.2.2	River Don flood 2007, UK	47
3.3	A portfolio of Nature Based Solutions –NBS	51
3.3.1	River Glinščica	51
3.3.2	River Don	51
3.4	Cost-effectiveness analysis viewed as square-lake graphs	53
3.4.1	River Glinščica	53
3.4.2	River Don	57
3.5	Limitations, extensions and inclusion of uncertainty	61

4	Wetropolis flood demonstrator	65
4.1	Tour of Wetropolis	65
4.2	Modelling Wetropolis: designing versus predicting	65
4.2.1	Saint-Venant equations	65
4.2.2	Design model	66
4.3	Extreme Wetropolis' floods	66
4.3.1	Design model results	66
4.3.2	Predictive model results	66
4.4	Flood-excess volume and square-lake graphs	66
4.5	Outlook: data assimilation and flood control	66
4.6	Redesign	66
	Appendix: Numerics	66
4.6.1	Design model	66
4.6.2	Predictive model	66
5	Discussion and outlook	67
	References	68

Acronyms

AEP	Annual Exceedance Probability
BCR	Benefit Cost Ratio
BD	Beaver Dams
CBA	Cost Benefit Analysis
DTM	Digital Terrain Model
EA	Environment Agency (UK)
EU	European Union
FEV	Flood-Excess Volume
FPS	Flood-Plain Storage
GRR	Giving-Room-to-the-River
HW	Higher Walls
LCC	Leeds City Council
M	Million
NAIAD	“NAture Insurance Value: Assessment and Demonstration” –EU project
NBS	Nature Based Solutions (to flooding)
NFM	Natural Flood Management
OB	Onno Bokhove –the author’s name
RFV	“Rainfall fraction” vector
SCC	Sheffield City Council
UK	United Kingdom
USA	United States of America

Chapter 1

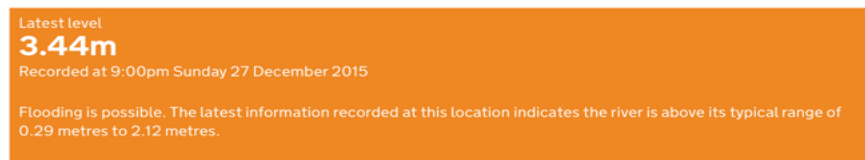
Introduction

Abstract The devastating Boxing Day floods of 2015, as well as the Storm Ciara floods in February 2020, both in Yorkshire, UK, triggered most of the work described in this brief, including actual flood evacuations in which the author was involved. The Boxing Day floods of 2015 therefore form the starting point to introduce several questions considered on the mathematics of river flooding. After briefly discussing the extent to which rainfall/precipitation and extreme flooding has changed in the last few decades due to climate change, the two key questions to be addressed in this brief are posed: how can we explain the magnitudes of extreme river floods to the general public and how can we communicate flood-mitigation plans to the people, from engineering experts and decision makers to the general and affected public, and effectively involve them all?

1.1 Questions on flooding: background and history

The Boxing Day flood of 2015 in Leeds, UK, was the worst flood on record the city's history with water levels of the River Aire, which flows through the city, exceeding those of the 1866 flood, see Figs. 1.1 and 1.2. December 2015 was the wettest month on record. Prior to and during this Boxing Day flood it had rained heavily and nonstop for 48hrs. Bingley, 13mi upstream of Leeds, saw 94mm of rain and Bradford, 9mi upstream from Leeds, saw 69mm of rain in these 48hrs [16, 28]. The floods of 2015 caused widespread damage in Yorkshire, UK, around £500M [49], caused by extreme and high water levels of three West Yorkshire rivers, the River Aire and River Calder, as well as the River Wharfe, respectively. The magnitudes of these extreme floods were ranked by their return periods as circa 1:200yr, or higher, for the River Aire in Leeds and circa 1:100yr for the River Calder in Mytholmroyd. Alternatively, their Annual Exceeding Probabilities (AEPs) were 0.5%, or less, and 1%. Such rankings tend to be based on records of (electronic) river-level measurements at selected spots along the river. The notion of return periods or AEPs often leads to confusion, also with the general public.

On the morning of Boxing Day 2015 (26-12-2015) river levels along the River Aire in and upstream from Leeds were rapidly rising from their already intermediately high levels, caused by the wet November and December months of 2015 [16]. The soil in the Aire catchment was saturated causing a fast response of the river levels to rainfall. It is and at that time was easy to follow the (changes in) river levels since the Environment Agency (EA) maintains a publicly-accessible online network of river gauges in England, with recordings at circa 15min intervals¹. River levels provided at Crown Point, Armley and Kirkstall Abbey can thus be followed in Leeds as well as upstream river levels at Apperley Bridge (9mi), Saltaire (13mi), Bingley (15.5mi), Kildwick (24mi) and Skipton (30mi –distance measurements in milage along the Leeds–Liverpool canal, a canal that partly follows of the River Aire valley).



5-day information for this station

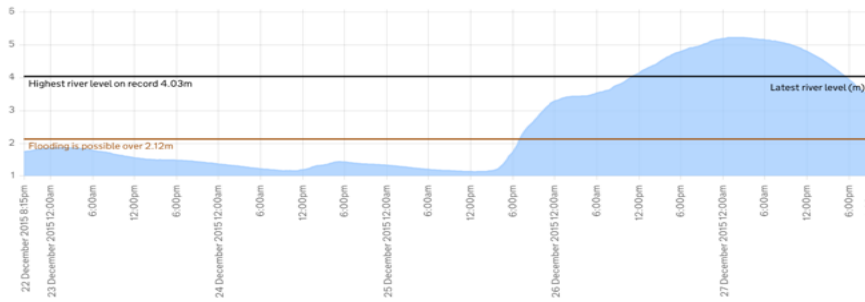


Fig. 1.1 Water level versus time for a few days prior to and during the Boxing Day floods 2015, data as displayed on the publicly and online available Armley river gauge at 9pm on 27-12-2015, are shown. Screenshot by OB.

It had started raining on 25-12-2015 and except for a lull in rainfall intensity and river-level rise at night, it continued to rain heavily. This was confirmed by looking outside and matched accompanying forecasts broadcasted by the BBC. River levels were seen to rise at a rate of circa 0.15m/hr, see Fig. 1.1. To assess whether minor or major flooding is expected to occur at a certain location one needs to estimate or

¹ E.g., google “river level Armley, Leeds” and several links to this online network will emerge; recordings stored over a few days are often made available online within 15 to 30min. E.g., Fig. 1.1.

know the critical or threshold h_T of the in-situ water level, the latter denoted by $h(t)$ as function of time t .

Attention was focussed at the Xfit-the-Forge gym on the Kirkstall Industrial estate due to my familiarity with this location, see Fig. 1.3a). This gym is located upstream of Leeds' city centre and about a mile upstream of the steep and high Dark Arches' weir under the railway station. These qualifications "steep" and "high" are essential in that this weir constitutes a hydraulic control point, especially during (extreme) floods. Water levels downstream of the Dark Arches' weir do not affect water levels upstream of the weir, while during high water levels nearby (natural) rapids submerge and the weir controls the water levels a few miles upstream, including the water levels at the Kirkstall industrial estate and the nearby Armley river gauge, see also the remark by the EA on the Armley river gauge, e.g., see [4] and images therein. Information in a river travels according to signal speeds or "lambda's", defined by $\lambda(s, t) = |u(s, t)| \pm c_g(s, t)$, involving the water velocity $u(s, t)$ and the gravity-wave speed $c_g(s, t) = \sqrt{gh(s, t)} > 0$ (the square root of the acceleration of gravity times the water depth), with water depth $h(s, t)$ and acceleration of gravity $g = 9.81\text{m/s}^2$, as as function of time t and location s along the river. Either cross-sectional averages or maximum values are used for water velocity and water level. The gravity-wave speed c_g is essentially the speed with which surface waves on the river surface travel, for small-amplitude surface waves. When the flow speed is less than this gravity-wave speed, such that $|u| < c_g$, no information can travel upstream and the flow is called subcritical. When the flow speed is larger than this gravity-wave speed, such that $|u| > c_g$, information can travel upstream against the current and the flow is called supercritical. At the Dark Arches' weir in Leeds there is a subcritical-supercritical-subcritical transition with critical control points, where the flow speed equals the gravity-wave speed, such that $|u| = c_g$, at the top and bottom of this weir. The weir itself is fixed dam at the entrance tunnels of the Dark Arches, raising the river levels upstream of the dam, followed by a long and steep decline through the tunnels of the Dark Arches in the downstream direction.

The above hydraulic considerations matter because one needs to establish whether the readings of the water levels at nearby river gauges are relevant for the potentially flood-affected location of relevance, here our chosen location at the Xfit gym in Kirkstall. The Armley river gauge lies within a few hundred metres from the Xfit gym and the flow is subcritical when the river is in flood. The gauge level is then controlled by the water level set at the top of the Dark Arches' weir.

One further needs to assess whether flooding at the Xfit gym is caused by the river overflowing the banks directly near the gym or along a stretch further upstream with waters approaching the gym via a normally-dry Kirkstall Road, or both? Without detailed Digital Terrain Model (DTM), observations and/or accompanying computer simulations a precise assessment is difficult to make. However, about 1km along Kirkstall Road, the river is closest to the low-lying Kirkstall Road next to a car wash/petrol station. The flooding of Kirkstall likely commenced here –see also the remark by the EA in [15]. Mid December 2015 river levels reached a height of circa 3.8m on the Armley river gauge and the gym owner reported that the river could still rise about 0.5m before it would have overtapped the banks at the footbridge near the



Fig. 1.2 Plagues at Leeds' Armley Industrial Museum displaying the highest river levels for the 1866 and 2015 River Aire floods, with Craigh Duguid's length –with permission- providing a scale for comparison. Courtesy: photo by OB, used before in [4].

gym. Given the lower river bank further upstream and this information, the threshold for flooding of the gym was thus estimated conservatively at $h_T = (3.9 \pm 0.2)\text{m}$ on the Armley river gauge with the error bars being an educated or a mere guess.

Around 9am on Boxing Day 2015, the water level at the Armley river gauge was circa 3.7m and rising at a speed of circa 0.15m/hr, so given our choice above of $h_T = 3.9\text{m}$, flooding at the Xfit gym was expected to start in about two to three hours. Around noon flood waters had risen to the front of the gym at circa 4.16m on the Armley gauge (see the time-stamped photographic evidence of a gym member in Fig. 5 of [4], which was matched to the river gauge-level closest to that time). From 3pm onwards, an evacuation crew of eight people brought circa £20k of gym equipment to safety at higher levels, which evacuation was halted at 6pm when water levels had risen to circa 4.7m, about knee deep in the gym and hip deep when this evacuation crew had to wade through the torrent of flood waters along Kirkstall Road in order to reach dry land. Water levels rose to a record level of 5.22m at circa 1am just after midnight on the Armley gauge. The above water levels emerge from the Armely gauge information displayed on 27-12-2015, as can be verified from the screenshot in Fig. 1.1 as well as the detailed data record one can obtain from the EA –data used in our programs at <https://github.com/Flood-Excess-Volume/>.

The EA triggers an amber flood warning when river levels rise above 2.7m on the Armley river gauge for the Kirkstall industrial estate. For most businesses that level and slightly higher levels neither lead to flooding of their premises nor any flood damage. For the Xfit gym, the above fluid-dynamical considerations combined

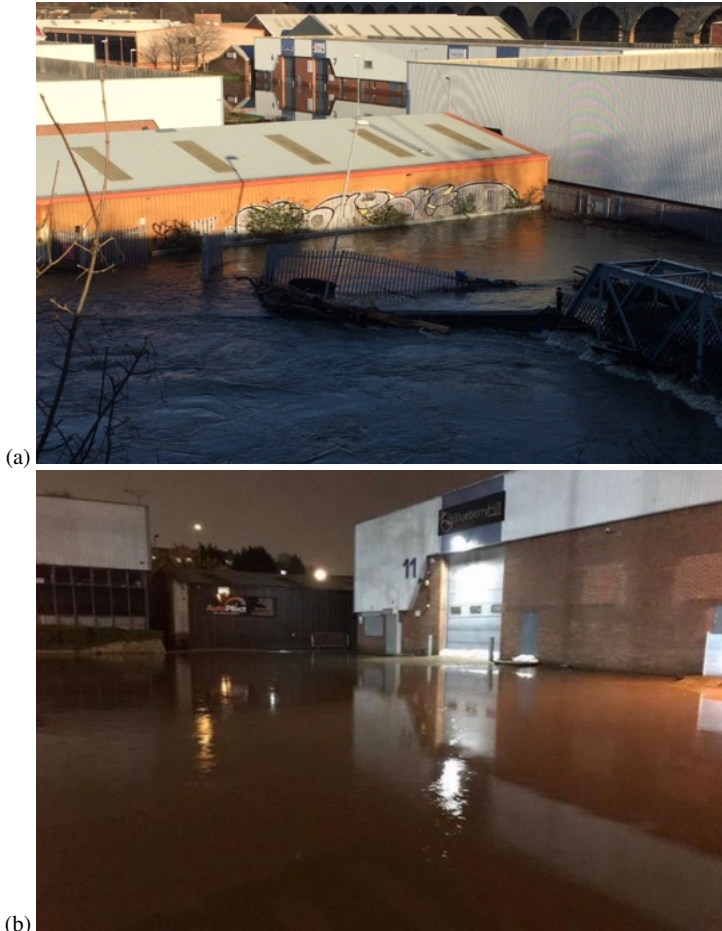


Fig. 1.3 (a) Photograph by OB of the Kirkstall Industrial Estate, including the parking lot in front of the Xfit The Forge gym during the Boxing Day floods on 27-12-2015 at 13:08:43 with level at circa 4.6m. (b) Photograph during the Storm Ciara flood on 09-02-2020 of the studios at unit 11 across the road from the Xfit gym at circa 18:00 with a 4.13m. Photo courtesy: Mike Rawlinson.

with the eye-witness information of the gym owner and EA data records of mid December 2015 triggered the impromptu flood-evacuation performed on Boxing Day after my warnings. The plan was formalised in December 2015 after the flood, using a threshold flooding level at $h_T = 3.9\text{m}$, somewhat below the 4.16m when flood water entered the streets in front of the Xfit gym. It included both instructions on timings, by using the rise per (quarter of an) hour from the 15min-interval recordings of the Armely river gauge levels as well as instructions on where gym equipment could be stored at safe higher levels in the gym. This formalised plan was again used by the Xfit gym in a 90min evacuation during Storm Ciara in February 2020,

after I had warned the Xfit owner and coaches, who had shared the evacuation plan and its timings with adjacent businesses. While flood levels fell circa 0.10m short of flooding the Xfit gym during Storm Ciara, nearby businesses experienced minor flooding yet managed to evacuate equipment in time [21]. Peak levels on the Armley gauge reached 4.13m, see Fig. 1.3b). The Boxing Day flood of 2015 had a return period of circa 1:200yr (EA's first estimate in 2016 was slightly higher, whereas [16] notes that no return period can be given based on the statistical method used and [30] states a 1:200yr return period), while the flood during Storm Ciara had a return period of circa 1:30yr, i.e. AEPs of circa 0.5% and 3.3%, respectively (see Table 3.4 in [30]).

In 2015, the EA provided an amber-alert (minor) flood warning at a lower river level, i.e. 2.12m, see Fig. 1.1, and a red-alert flood warning at a higher water level, an amber-warning threshold level raised after the Boxing Day flood to 2.7m. In my evacuation plans, I had augmented these EA warnings by combining hydraulic insights with knowledge of the local terrain, prior observations of water levels — official, photographic and reported ones— as well as the Armley river-gauge levels and their changes during a flood, in order to obtain the amount of time one has to evacuate and save goods (and lives) for the in-situ and chosen location, after an estimate of the flooding threshold h_T had been established. One can raise the question whether every household and business in a flood plain should or could make such a flood-evacuation plan including timings such as to refine the EA warning system [21]? Should people be responsible to acquire the skills to make and use such timings or should such a more bespoke and refined system of warnings and timings be developed for them, using river gauge levels, time-stamped visual flood data from citizens, DTMs etc.?

The above flood events and similar evacuations across Yorkshire and the UK led many people to raise further questions, some of which triggered the outreach and research described in the forthcoming chapters:

- To what extent have extreme rainfall/precipitation and flooding events increased in the last few decades?
- How can we explain return periods or Annual Exceedance Probabilities (AEPs) to an interested general public, including decision makers?
- What is a good way to communicate and improve flood-mitigation plans including facilitation of interactive discussions with this general public?

To answer the first question on precipitation increases, the report of the Intergovernmental Panel on Climate Change (IPCC) [46] as well as the 2009/2010 UK Met Office report [43] reveal that there is no significant annual increase observed in climate projections on precipitation, either globally or locally in the UK on average. There are, however, both spatial and temporal variations and an increase in the occurrence of extreme events in precipitations, with therefore average winter precipitation increases and summer precipitation decreases but with heavier downpours seen during the summer. Furthermore, the more recent 2018/2019 UK climate projection report of the Met Office [27] does reveal an increase in annual rainfall over the last decade (2008–2017) with natural variations found in the longer observational

record. In addition, the latest IPCC report of 2021 increases the warnings given in the 2013 report of the IPCC. Consequently, an increase of extreme flooding events is forecast in climate projections which matches the extreme water-level records seen during floods in recent decades, in the UK, e.g. during the 2015 and 2019 floods in Yorkshire. Overall, probabilistic projections of [43] overlap with those in [27] with differences in the tails of the climate projections, i.e. regarding the occurrences of extreme rainfall events. The 2010 report [43] contains valuable graphs showing how return periods of extreme events decrease in climate-change projections, with large uncertainties in these projected decreases for the high-return-period events. The extensive answers to the last two questions on return periods and communication will comprise the content of what follows.

1.2 How do we explain return periods to the general public?

In November 2019 the River Don, UK, severely flooded, with extensive damage in the towns of Doncaster and Fishlake as well as record river levels, twelve years after the 2007 floods that severely devastated the city of Sheffield, including several casualties. In a radio interview during these 2019 floods, someone expressed surprise since the magnitude of these 2007 River Don floods were rated as 1:100yr floods and therefore this person had not expected such flood levels for circa another 100 years. It is a common misconception to associate such return-period ratings with floods that regularly return with roughly the return period as time interval between subsequent floods. For the River Don case that led to the misconception with the person interviewed that a 1:100yr return period flood occurring in 2007 would not occur again till around 2107, i.e. roughly 100 years later. Of course, that is not what a return period means, since the 100 years indicated merely denotes the average time interval between floods of that 100–year magnitude under the assumption of statistical stationarity. Perhaps the use of Annual Exceedance Probability (AEP) is better, with $AEP = 1\%$ for a 100 year return-period flood, at a certain location, meaning that there is a one percent or $1/100$ chance that a flood of such magnitude occurs per year. Explaining return periods or AEPs to the general public, including sometimes also decision makers, is generally perceived to be difficult. After the Boxing Day floods, various flood professionals and citizens' flood-action groups had asked me the question whether it was possible to explain or even visualise return periods, preferably in a demonstration rather than a computer model. Attempts to address that question leads to the work reported in this brief.

Let us assume that we have a 1000yr record of River Don floods. Two (fictitious) realisations of such floods with an $AEP = 1\%$ (i.e. of one percent), including the known recent ones in 2007 and 2019, could for example be the following:

$$\{1303, 1376, 1707, 1811, 1823, 2007, 2019, 2050, 2100, 2295\}$$

or



Fig. 1.4 (a) The coastal wavetank, commissioned by JBA Trust and designed by Centre of Doctoral Training (CDT) students Jacob von Alwon, Thomas Goodfellow and William Booker in a 2015 MSc project (Leeds' CDT in Fluid Dynamics), demonstrates how different types of coastal defences lead to different levels of overtopping and coastal protection. See also <https://www.youtube.com/watch?v=3yNoy4H2Z-o>. Courtesy: wavetank with blue-dyed water, waves splashing against a coastal defence on the left and wave generator on the right (top), by JBA Trust, and wavetank at rest with the various types of insertable coastal defence walls (bottom), by Thomas Goodfellow. (b) Two snapshots of the Hele-Shaw wavetank consisting of two glass plates, spaced 2mm apart, filled with water and particles (diameter 1.8mm) and a drill-operated pump that sends water periodically in and out of the tank. A beach is formed due to the interaction with the water waves (bottom right). The waterline is highlighted in white and the top of the particle layers in red. See also [31], https://www.youtube.com/watch?v=iz_S-NILYyU and <https://www.youtube.com/watch?v=UYhgxUMKBQ0>. Photos by the author.

$$\{1407, 1553, 1544, 1717, 1717, 1823, 2007, 2019, 2210, 2221\},$$

in which we somewhat artificially used 10 events even though one needs a longer record to reach the average of a flood once every 100 years. In addition, in the second flood sequence, two flood events of that magnitude occurred in the year 1717. Albeit less likely, that can occur. Perhaps it is easier to explain a river flood at a certain location with a large $AEP = 50\%$, i.e. a flood with a magnitude that occurs on average every two years, yielding a 1:2yr return period. For simplicity, let us assume only one such flood can occur in a year such that a flip of a perfect coin would determine the AEP for that river for a given year. One can easily generate a few realisations, say three: (i,ii,iii), with a length of 10 years, say, e.g.: (i) {1, 1, 0, 0, 1, 0, 1, 0, 1, 0}, (ii) {1, 1, 0, 0, 0, 0, 1, 0, 0}, (iii) {1, 1, 1, 1, 0, 1, 1, 0, 0, 1}, etc. in years 1 to 10. These three realisations resulted from me actually flipping a Euro coin for 3×10 times with heads/floods denoted by 1 and tails/no-floods by 0. The first realisation has the same number of floods and no floods (of that $AEP = 50\%$ —magnitude), the second one has only three floods and the last one seven floods with somewhat fortuitously the average across the three realisations still being 50%. With a standard and perfect dice with six sides, one could also make other realisations, e.g. for $AEPs = 16.6\%, 33.3\%$ —or $1/6, 1/3$ —which are smaller than $AEP = 50\%$ or $1/2$. An ideal dice with 100 faces could be used to generate realisations for floods with an $AEP = 1\%$. While illustrative to explain basic statistics, these ways to practically realise AEPs are not very useful because a binary division between a flood with a certain magnitude or AEP and no flood is unrealistic. In reality, one needs to consider a variety of floods of different magnitudes, such that the relative distribution between floods needs to be obtained, either theoretically or based on a data record, or preferably both. An ideal or sufficiently long record of extreme rainfall or flooding events can be used to make a histogram of the number of events versus a binning into intervals with certain rainfall amounts or a floods magnitudes. Subsequently, this can be turned into AEPs to classify extreme events. In the above examples, the statistics for a flood or rainfall event were considered at a specific location under the assumption of stationarity, e.g. without the nonstationary effects of climate change. Further statistical complications arise because a river flooding a city is affected by the temporally varying rainfall distributed over all relevant, constituting a continuum of, locations. The pathways along which the rain water travels before it can flood this city are varying in space and time. Such paths involve groundwater, surface and channel flows through and over more or less porous soil (e.g., through woods, in urban or rocky areas). It means that the statistical distribution of the flood in the city will be a different composite of the spatio-temporal rainfall distributions involved. The Boxing Day 2015 flood was a case wherein this composite was relatively simple since the soil was saturated by the heavy November and December 2015 rainfall such that the river levels were quite directly responding to the incoming spatially fairly uniformly-distributed rainfall. The statistics of floods is further complicated by the limited data records we have of floods. For floods with a large return period, reletative to the length or the record, or beyond that length, the return period can only be estimated based on extreme-value theory using theoretical statistical distributions with an exponential tail [14]. The

Wetropolis flood demonstrator was born as a simplified yet live visualisation, of such complicated statistics involved in extreme rainfall and flooding events. It was designed to enlighten the general public.

The design of Wetropolis benefitted from experience gained in two other demonstration models of environmental fluid dynamics which I have initiated and co-designed: the coastal wavetank demonstrating the effects of various types of coastal defences on incoming waves and the Hele-Shaw beach generator demonstrating how incoming waves create various types of beaches, see Fig. 1.4.

Wetropolis is designed based on a simplified mathematical and numerical model of the key features involved [5, 8]. A plan view of Wetropolis, given in Fig. 1.5a), shows that it involves an idealised meandering and slanted rectangular river channel (white-blue striped channel) with a one-sided slanted flood plain (between this river channel and the dashed line), upstream inflow, a porous moor visualising the possible delay of rainfall via ground water flow into the river channel, a reservoir that can store some rainwater or leads to direct runoff into the river channel, a conceptual city downstream that can flood under extreme rainfall, as well as an outflow point. Water can enter Wetropolis at three points: as constant inflow upstream, as temporally and spatially varying rainfall onto the moor or into the reservoir, which exits are located about one-third or two-thirds along the main river channel. A mathematical *design model* (as opposed to a *predictive model*) was used to determine the strengths of the three required pumps feeding the water into Wetropolis at these three locations as well as the length of a *Wetropolis day* (with a hypothetical “SI” unit denoted by “wd”). Rainfall onto moor and reservoir varies in magnitude, e.g., it can fall during (10, 20, 40)% or 90% of a wd, and location, e.g., it can fall onto the moor or reservoir, both, or not rain at all. The statistics of each of these four outcomes are generated via altered, skew-symmetric Galton boards, that generate varying water levels in the city and, by design, rare-event flooding of the city through 4×4 spatio-temporal rainfall outcomes, see Fig. 1.5b). The mathematical design model has been tuned such that an audience does not have to wait 100 years on average, such a long wait on average is deemed undesirable, for an extreme flood event to happen in the city. Instead the Wetropolis day has been shortened to $wd = 10s$, rainfall is localised and intensified to two spots instead of spread out over the catchment to avoid water splashing everywhere, and the return period is by design shortened to a handful of minutes. Hence, Wetropolis provides a conceptualisation of extreme rainfall and river flooding. Extreme flooding in Wetropolis remains random, however, such that the viewer experiences both what a rare event is by typically having to wait a few or two handfuls of minutes. Its rare event is random because the rainfall driven by the Galton boards coupled to the moor and reservoir visualises what spatio-temporal randomness signifies in outside-world extreme events.

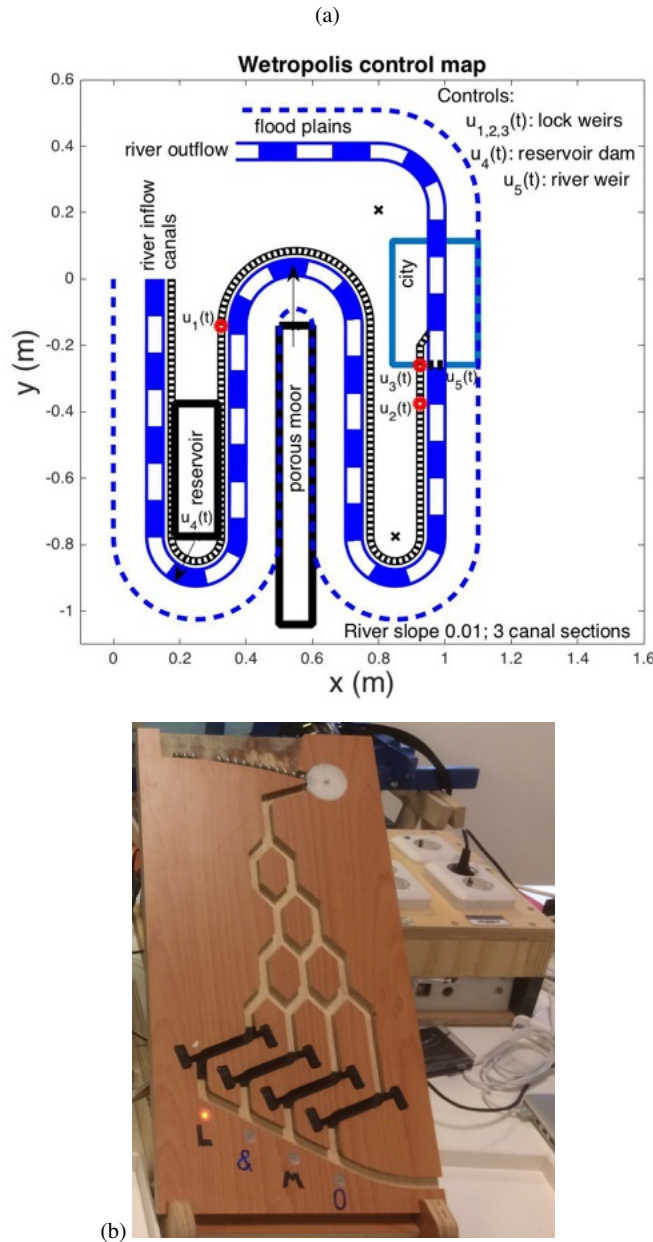


Fig. 1.5 (a) Overview of Wetropolis flood demonstrator. Figure 2 of [5], reproduced with permission. (b) Skew-symmetric Galtonboard: a steel ball falling through determines four outcomes, in the ideal case with a 50% chance of the ball to fall left or right per split the outcomes are distributed from left to right as $(3, 7, 5, 1)/16$ – it is a fun calculation to check these outcomes.

1.3 How do we communicate flood-mitigation plans?

Consider a village intermittently flooded when the brooke flowing past the village bursts its banks. Just upstream of the village there is a bridge across the brooke. A playing field flanks the brooke upstream of this bridge, separated from the brooke by small earthen berms along the stream. The villagers are wondering whether the playing field holds sufficient volume to function as flood-storage buffer to alleviate future flooding of the village. There is no river-level and flow-measuring device installed along the brooke but there is some camera footage of the maximum water level reached at the bridge during flooding events of the village. The village flood-action group therefore decides to install a vertical stick with markings at the bridge as well as a camera recording what the river level along that marker is. Furthermore, a device recording the water-level relative to the ceiling of the bridge is installed. Such devices are now available, (relatively) affordable and promoted in citizen-science projects. In addition, the bed profile must be measured under the bridge, also relative to the marking stick and the ceiling of the bridge such that these measurements can be related to the (mean or maximum) water depth $h(t)$ as function of time, but luckily the cross-section is pretty much rectangular. To get estimates of the discharge $Q = Q(t) = Q(\bar{h}) = Q(\bar{h}(t))$ in cumecs (cubic metres per second or m^3/s) at higher water levels, surface velocities across the brooke are obtained by throwing in floating objects such as Poohsticks or oranges and timing their passage under the bridge using repeat measurements². Given the width of the bridge W_b and time of passage T_p of a Poohstick, one can obtain surface-velocity measurements

$$V_s = W_b / T_p, \quad (1.1)$$

in m/s, and further compute the mean surface velocity, as well as an error estimate thereof, from multiple such measurements in a sufficiently short span of time for which the discharge barely changes. Subsequently, an approximation of the discharge is found by integration or even more simply by using the mean of the velocity profiles and the mean depth. However, then one needs the mean of these quantities. Given the rectangular cross-section $W_b h$, expressed in m^2 , and surface velocity V_s , expressed as m/s, and assuming that the flow is turbulent at higher flow rates and therefore approximately depth-independent, the discharge can be estimated directly as follows

$$Q(h) \approx K W_b h V_s. \quad (1.2)$$

² “He [Pooh] had just come to the bridge; and not looking where he was going, he tripped over something, and the fir-cone jerked out of his paw into the river. ‘Bother,’ said Pooh, as it floated slowly under the bridge, and he went back to get another fir-cone which had a rhyme to it. But then he thought that he would just look at the river instead, because it was a peaceful sort of day, so he lay down and looked at it, and it slipped slowly away beneath him . . . and suddenly, there was his fir-cone slipping away too. ‘That’s funny,’ said Pooh. ‘I dropped it on the other side,’ said Pooh, ‘and it came out on this side! I wonder if it would do it again?’ And he went back for some more fir-cones. . . . And that was the beginning of the game called Poohsticks, which Pooh invented, and which he and his friends used to play on the edge of the Forest” [29]. Oranges are better than sticks since they are more visible and mostly submerged and thus less prone to drift by the wind.

The K -factor herein arises as a dimensionless scaling factor with $K \in [0.65, 1.0]$, see [37], in which discharge calculations with these easier-to-make surface velocity measurements have been compared with more advanced velocity-profile measurements in order to determine K and assess its range.

The next step is to choose a (range of) relevant threshold level(s) h_T for which it is known that minor, intermediate or major flooding in the village occurs. Subsequently, either by using knowledge of the water level as function of time for previous flooding events or by attaining this knowledge for new flooding events, the flood duration needs to be established. For a chosen threshold level h_T on the scale installed at the bridge, the rising time t_{ri} and receding time t_{re} at which the water level equates this threshold, $h(t_{ri,re}) = h_T$, both for rising and receding water levels, need to be found. The flood duration, $T_f = t_{re} - t_{ri}$, for that chosen threshold is the time difference between these two times. Notice that this flood duration is, of course, a function of the chosen threshold, which is expressed as $T_f = T_f(h_T)$. When one chooses a higher threshold level, then the flood duration will decrease and become zero when the threshold equates the maximum water level attained. For certain thresholds and floods, multiple flood peaks emerge with multiple rising and receding pass-through times such that the above calculation of flood duration needs to be adapted to one with T_f the sum of multiple flood durations over the peaks associated to one flood.

Assuming that the maximum surface velocity V_{max} and maximum depth h_{max} have been measured, then the peak discharge $Q_{max} = KV_{max}W_b h_{max}$, which has units of cubic metres per second, in short “cumecs”, given that velocity has as units metres per second, while the width and water levels have metres as unit. The volume of flood water that causes the flood damage equals the discharge above the threshold level $Q_T = Q(h_T)$. If we would know the mean water depth during flooding then the mean discharge $Q_m = Q(h_m)$ depends on the mean water level h_m . Given the duration over which the water levels are above the threshold level h_T , an estimate of this “flood-excess volume” (FEV), denoted by V_e and causing the flood damage, is by definition as follows

$$V_e \approx T_f(Q_m - Q_T), \quad (1.3)$$

i.e., the flood duration T_f times the difference of the mean discharge Q_m and the threshold discharge Q_T . When the relationship or “rating curve” $Q(h)$ between discharge Q and water depth h is approximately taken to be linear such that the discharge at a given water level is the fraction $Q(h) = Q_{max}h/h_{max}$ of the measured maximum discharge, then

$$Q_m = Q_{max}h_m/h_{max} \quad \text{and} \quad Q_T = Q_{max}h_T/h_{max}. \quad (1.4)$$

For a rectangular hydrograph, the discharge $Q(t)$ as function of time, for which $h(t)$ is then also rectangular, given that $Q \propto h$ for a linear rating curve, we find that $h_m = h_{max}$. For a triangular hydrograph and linear rating curve, again $h(t)$ has the same now triangular shape, one finds that $h_m = (h_{max} + h_T)/2$. Hence, the FEV approximations using (1.3) thus become

$$V_e = T_f Q_{max} \frac{(h_{max} - h_T)}{h_{max}} \quad \text{and} \quad V_e = \frac{1}{2} T_f Q_{max} \frac{(h_{max} - h_T)}{h_{max}}, \quad (1.5)$$

respectively, for the rectangular and triangular hydrographs. E.g., when taking $W_b = 1.5\text{m}$, $V_{max} = 1\text{m/s}$, $h_{max} = 1.2\text{m}$, $K = 0.8$, $h_T = 0.9\text{m}$, $T_f = 10\text{hrs}$, one obtains

$$Q_{max} = 1.44\text{m}^3/\text{s} \quad \text{and} \quad V_e = 6480\text{m}^3. \quad (1.6)$$

In order to store that excess volume V_e , the playing field also earmarked for flood-storage therefore needs to have a size of $114 \times 114 \times 0.5\text{m}^3 = 6498\text{mm}^3 \approx V_e$, i.e. it is a square lake with equal sides of length 114m and depth 0.5m, assuming that such field is available for extra water storage. When the field is already flooded prior to any new flood-mitigation intervention to create extra storage, the water levels need to be raised artificially by an extra 0.5m to buffer the flood, e.g. via a dynamic weir. A weir is a dam in the river stowing up its waters over which the river flows. Dynamic weirs concern the case for which the dam height can be altered, for example a door constrained to move vertically, with water either flowing over the door or under the door –so-called overflow or underflow weirs, respectively. Alternatively, when the field was dry prior to such an intervention it needs to be made available for this storage. If only only a fraction of V_e can be stored since the playing field does not have sufficient capacity then other flood-mitigation measures may be needed, for example the erection or raising of flood-defence walls or earthen bunds, which effectively increase the threshold height h_T for flooding to occur³.

In general, people may have little sense of the size of a flood and the relative merits of flood-mitigation measures, also in comparison to the size of that flood. What the above example demonstrates is how one can obtain a sense of size, of the flood-excess volume V_e , water-level and discharge thresholds h_T and Q_T , and flow speeds such as V_{max} by fairly straightforward measurements and estimates. Herein, note that the flood-excess volume V_e is the volume one wishes to reduce to zero to avoid the flood damage for floods with a similar magnitude. Subsequently, one can assess what fractions of this flood-excess volume can be mitigated with the various available mitigation measures, introduce their costs, make comparisons and explore different mitigation scenarios. Such science-policy explorations are important to enhance the communication with and interactions amongst flood-action groups, decision-makers and flood professionals in order to improve flood-protection schemes. The latter improvement is important in an age of increasing weather extremes under climate change [43, 27].

³ I have included these paragraphs on “Poohsticks” [29] to stimulate private citizens to take hold of their own situation in villages with intermittent flooding where official and/or government data are lacking. It was inspired by the Churchtown Flood Action group who had invited me to speak on extreme flooding and to showcase the Wetropolis flood demonstrator at their insightful conference in January 2017.

1.4 Outline

The straightforward example given above of flood-mitigation planning for a village shows that there are a range of measurements and considerations involved in such planning. In chapter 2, various flood data, rating curves and hydrographs are introduced based on more advanced, electronically-available measurements for a variety of real river-flood data. The concept of flood-excess volume will be formally defined and a range of storage-based flood-protection measures will be introduced. In the above example of the brooke flooding the village, the efficacy of the playing field as flood-storage site depended on whether the playing field was already flooded prior to its role as storage site for floods of similar magnitude. Inherent in this discussion lies the relatively new or rephrased concept of available flood-storage volume. That concept will be defined and subsequently considered in different flood-control strategies of dynamic flood-storage, one for beavers and one for humans who have different goals and, hence, use different cost functions. The reintroduction of beavers has been hailed in the UK, including in the media, while often emphasising the beavers' potential role in preventing floods. Using the concepts introduced hitherto of flood-excess volume for various river floods and flood-storage volumes involved in beaver-dam complexes, it is straightforward to show that this potential is minimal to minute. The reasoning and data involved herein serve as an insightful example in understanding several mathematical and hydraulic concepts in flood mitigation.

Expressing the flood-excess volume as a square lake with equivalent volume has led to the development of a graphical cost-effectiveness tool for flood mitigation [3, 4, 21, 9]. Such square lakes, including the square lake in the example of the flooded village, tend to be very shallow or thin compared with the side length when the lake depth is chosen to have a human scale of 0.5 to 2m. Consequently, the lakes can be viewed as square pies or piecharts. Different flood-mitigation measures will cover the entire square lake in segments and when the entire square lake is covered future damage (for floods of similar magnitude) will be lessened or prevented. Given that the size of the square lake relates to the size or rather flood-excess volume of a flood, each mitigation measure has significance as a fraction of that volume. When costs of each measure and total costs are overlaid, costs and effectiveness are combined. Hitherto, the tool has been applied, and subjected to peer review, to understand mitigation for the River Aire in and upstream of Leeds [4], to develop mitigation plans for the River Brague in a French municipality [39, 3, 9] after devasting floods in 2015 as well as in communicating nature-based-solutions (NBS) to flooding in Slovenia [39, 9, 36]. The cost-effectiveness tool is introduced in Chapter 3 by considering flood-mitigation options for the River Don in Sheffield, based on data of the 2007 and 2019 floods, and by extending the discussion of NBS for the Slovenian River Glinščica near the city of Ljubljana. Both river cases include more and novel aspects of dealing with uncertainty in flood data and in (designing) flood-mitigation measures as well as dealing with the way we communicate this uncertainty. In addition, advantages and disadvantages of the cost-effectivess tool are discussed, leading to a new and more advanced protocol of flood-mitigation design and communication. Finally, note that the tool does not replace engineering design calculations of flood defences. Rather, it

encourages engagement of the general public and decision makers, and allows often complicated engineering calculations to be communicated and perhaps redirected as part of the overall (political) decision-making process involved in attempts to reduce the damage caused by (river) flooding.

An overview of Wetropolis based on various showcases, its inner workings, the details of the design model and a first more advanced predictive model are found in Chapter 4 as well as a discussion of possible improvements. What has come as a surprise is that both scientists and flood professionals found Wetropolis inspirational and thought that it should also be used as scientific experiment to advance and validate hydraulic modelling and data assimilation. This has been a surprise given that the original Wetropolis' aim simply was to visualise return periods to the general public. But then after all, the Wetropolis experience did stimulate the development of the science-policy work on the communication of flood-mitigation plans, as explained in Chapters 2 and 3.

Chapter 2

How do humans and beavers view river floods?

Abstract Advanced river-level and (intermittent) flow/discharge measurements are analysed for four river floods in particular. Where possible rating curves are introduced as a fit of water-level measurements versus discharge measurements. Flood-excess volume (FEV) is defined as the water volume causing the flood damage, based on introducing both water-level and discharge thresholds. Simplifications as well as complications in determining FEV are discussed. Various storage-based flood-mitigation measures are introduced, and exemplified visually by showing photographs, including higher defence walls, giving-room-to-the-river options, natural flood management, flood-plain storage and nature based solutions (to flooding). Herein the concept of available flood-storage volume is needed and thus defined. The potential of beaver dams for flood protection, or rather their lack of potential, serves as a nice first example of using FEV and available flood-storage volume. FEVs of a large number of river floods are presented and give a sense of the sizes of floods, relative to the size of the relevant river-valley landscape, for which the introduction of (dynamic) square lakes is and will become insightful. A more advanced mathematical example of available flood storage volume is crafted in an active or a dynamic control problem, involving a dam with adjustable porosity or gates permitting the control, in which both humans and beavers are seen to have different optimisation goals and cost functions.

2.1 Introduction

The do-it-yourself example described in the Chapter 1 introduced how one can measure water-level and discharge data in a case when there are no officially maintained river-gauge data of water levels and discharge available. In many countries, however, there is a network of river gauges set up across the country and either associated data are publicly available online, available on request, or both, with online data generally

given over a limited interval backwards in time¹. Data from these networks tend to be used in the forecasts of river floods. They are also used to monitor and maintain levels in navigation channels for shipping. In addition, while water-level data can be available online, discharge data tend to be measured less often, either directly or indirectly, which means that one needs additional, intermittently-measured data to convert water-level data, e.g., measured in metres (with unit m), into discharge data, e.g., measured in cubic metres per second (unit m^3/s or cumecs), at a given river cross-section. In England, the Environment Agency (EA) maintains such a network of river gauges with some of these data available online, while further information can (readily) be made available upon request under the Freedom-of-Information act.

In this chapter, such data measured by government agencies will be displayed, analysed and discussed for a variety of river floods, including the River Don in Rotherham Tesco (2019), River Ouse in York (2015) and the Tamar River in Gunnislake (2012), all in the UK, as well as the River Ciliwung near Djakarta (2020), Indonesia². These four rivers have been chosen because their data formats are different, regarding the directly measured river-level data, their rating curves and, hence, the way approximate discharge data are calculated. Furthermore, for each location it will be argued what threshold flood level h_T is chosen and why, whereafter the flood-excess volume (FEV) can be determined. A formal definition of FEV is provided, recalling its importance as the flooding volume that caused the flood damage, which when reduced to zero would in principle lead to flood protection for a flood volume recurrence of that magnitude. To get a sense of the size of floods, FEVs for a large range of floods will be summarised in a table for intercomparison.

Before the concept of available flood-storage volume is defined and discussed, an overview is given of a series of storage-based flood-protection measures. Beavers have been hailed as natural engineers who can (potentially) play a role in flood mitigation, both in some scientific literature and the (UK) media. The analysis of three beaver-dam complexes [40, 26, 48, 35] in three different rivers and their floods, in combination with the FEVs involved in a series of floods, shows that the potential of beaver colonies mitigating floods is rather limited. Nonetheless, such an analysis yields valuable insights in some (straightforward) river-flood hydraulics. It also triggers a brief investigation of mathematical flood control such as to either maximise or minimise the available flood-storage volume behind a porous dam with controls on its throughflow, operated by humans or beavers, respectively. Naturally, the reintroduction of beavers in the UK seems a good idea from a wildlife perspective even without the need to elude to the (minute) flood-mitigation potential by a multitude of beaver-dam complexes.

¹ E.g., Rijkswaterstaat The Netherlands:

<https://waterdata.wrij.nl/index.php?wat=standardgraph&deeplink=1>;

Environment Agency: <https://flood-warning-information.service.gov.uk/station/8184>; France.

² The initial data gathering and displays were acquired in student projects by Zheming Zhang (River Don), Antonia Feilden (River Ouse) and Nico Septianus (Ciliwung river), and by me (River Tamar). I have built on these projects and compiled material into one *Python* code.

2.2 River-level measurements

Water-level measurements are presented for four river floods in Fig. 2.2, concerning the November 18th 2019 of the River Don in Rotherham, UK, the January 1st 2020 flood of the Ciliwung river near Djakarta, Indonesia, the December 25th 2015 flood of the River Ouse in York, UK; and, the December 24th 2013 flood of the River Tamar, at Gunnislake, UK³. At the Tesco gauge, Depok Floodgate, Skelton and Gunnislake gauges the in-situ water depths $h(t)$ are measured at discreet time intervals t_k of time t with (regular) time intervals $\Delta t_k = 15\text{min}, 30\text{min}$ and 15min , respectively, for the first three gauges. The time interval at the Gunnislake gauge station is not given but daily mean, minimum and maximum water levels are reported by the EA. Note that the water-level is commonly measured relative to the deepest datum in the river's cross-section, which may change due to bed erosion and accretion, while the water-level marker or scale will stay fixed for a long time⁴.

The station information generally does not go into the details of what this reference datum is but given that the level-scale is fixed, cf. Fig. 2.1, small changes in its position relative to deepest riverbed point at a given cross section are irrelevant.



Fig. 2.1 Shown is the scale of the Ciliwung river in flood at the Depok Flood gate. Photo courtesy: Inews/Rizky [https://www.inews.id/news/megapolitan/pintu-air-depok-siaga-ii-warga-dibantaran-kali-ciliwung-diminta-waspada, see also Fig. 4.2 in \[44\].](https://www.inews.id/news/megapolitan/pintu-air-depok-siaga-ii-warga-dibantaran-kali-ciliwung-diminta-waspada, see also Fig. 4.2 in [44].)

The choice of the threshold h_T is open to some debate. Often the respective environment agencies provide thresholds for minor, intermediate and major flooding associated with a specific river gauge. It is important to have a clear rational for

³ <https://flood-warning-information.service.gov.uk/station/8175>,
e.g., <http://poskobanjirdsda.jakarta.go.id/Pages/grafikDataTinggiMukaAir.aspx>,
<https://flood-warning-information.service.gov.uk/station/8184>,
<https://flood-warning-information.service.gov.uk/station/3201>

⁴ For the Yangtze River, however, the river level is given relative to Chinese mean sea level at Wusong station near the city of Shanghai.

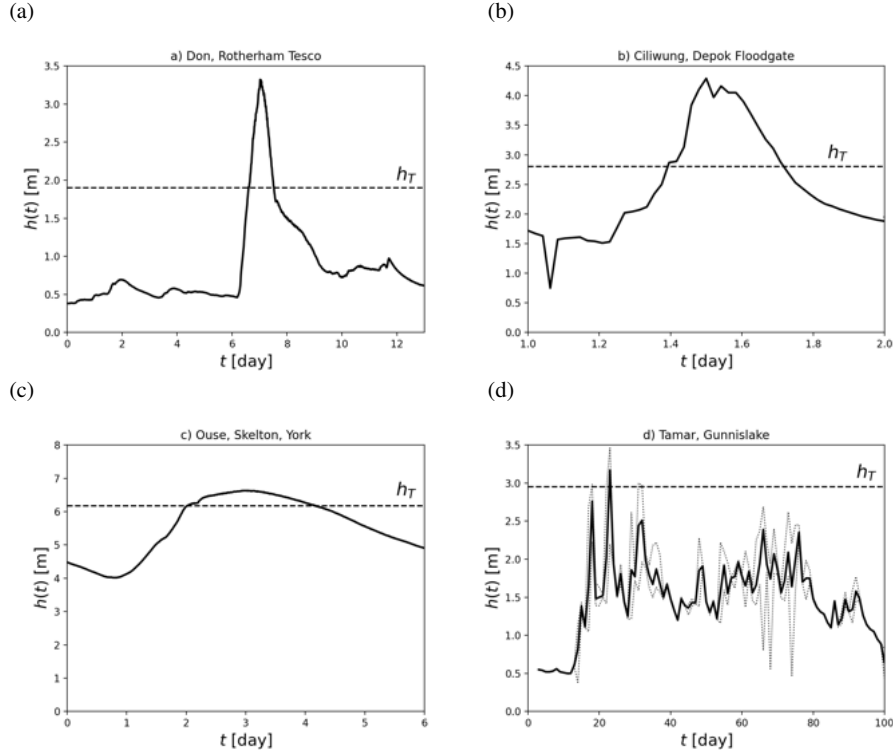


Fig. 2.2 Water-level measurements of water depth $h(t)$ versus time t for: (a) River Don 08-11-2019 flood at Tesco gauge station, Rotherham, UK, made every 15min; (b) Ciliwung river 01-01-2020 flood at Depok Floodgate gauge station near Djakarta, Indonesia, made every 30min; (c) River Ouse 25-12-2015 flood at Skelton gauge station, York, UK, made every 15min; and, (d) River Tamar 24-12-2013 flood at Gunnislake, UK, (minimum, mean and maximum) data collected per day. For the River Tamar the (daily) minimum and maximum (dashed, thin lines) as well as mean (solid, fat lines) water levels have been displayed.

the choice of h_T at each relevant location and to explore the effects of varying h_T , e.g., [4]. Bespoke local information can be added to the agencies' information based on eyewitness and/or photographic information. For the River Don case, the minor flooding threshold of 1.7m was slightly increased, yielding a choice of $h_T = 1.9\text{m}$. For the Ciliwung river, the above-mentioned Jakarta-flood website states specific river heights for the top two warning stages, as follows: a first, worst stage of overflowing and a second stage of initial flooding for $h > 2.8\text{m}$ and, hence, $h_T = 2.8\text{m}$ was taken. For the River Ouse, minor flooding near Skelton is possible for $h > 5.8\text{m}$. At the Viking-recorder-5 upstream, the EA reported flooding for $h > 4.55\text{m}$, which corresponded to a river level at 27-12-2015 of $h_T = 6.17\text{m}$ at Skelton (email of EA official to Antonia Feilden 19-03-2019). Finally, for the River Tamar the EA employs the following warnings: a flood alert at full banks is issued for a river level of 2.65m; a flood warning level is issued when $h > 2.95\text{m}$; and, a severe

flood warning is issued for levels over 3.45m, see [2]. Hence, a threshold value of $h_T = 2.95\text{m}$ was taken. Each threshold h_T is indicated by a horizontal dashed line in each panel of Fig. 2.2.

2.3 The role of rating curves

Rating curves convert water-level measurements to a discharge. In the simplest or ideal case, one water level $h(t)$ (expressed in m) corresponds to one discharge rate $Q(t)$ (expressed in m^3/s) across a river's cross-section, yielding a rating curve $Q(t) = Q(h(t)) = Q(h)$ at every time t . River dynamics is, of course, spatially three-dimensional and turbulent, especially during floods. However, for rivers with steeper bed slopes, one rating curve as one-to-one function between Q and h tends to be a good approximation. Rating curves are obtained by relating water-level measurements at a certain time with flow measurements at that time or over a sufficiently short time interval. By combining knowledge of the bed topography in that cross-section and these flow measurements (e.g. via usage of Acoustic Doppler Current Profilers –ADCPs, e.g., [32, 37]), one can approximate the discharge via integration of the velocity over the river cross-section, as follows

$$Q(t) \approx \int_{y_l(t)}^{y_r(t)} \int_{b(x,y)}^{b(x,y)+h(x,y,t)} V(x, y, z, t) dz dy, \quad (2.1)$$

with the y -coordinate aligned across the river, the x -coordinate in the local downstream direction and the locally vertical upward z -direction; the water depth $h(x, y, t)$ (assumed single-valued under no wave breaking or over a brief time interval); bed topography $b(x, y)$ (assumed steady over the time interval considered); $U(x, y, z, t)$ the local velocity component in the x -direction at a fixed location; and, with extent $y_l(t) < y < y_r(t)$. The time interval for velocity measurements must be sufficiently short such that the time dependence of $Q(t)$ is negligible. Velocity measurements are either taken over much longer time intervals (than the water-level measurements) or, occasionally, water level and discharge measurements are taken over the same time interval. In the former case, the results of such measurement campaigns generally accrue over days to months or even years such that one obtains a scatter plot of discharges for different water levels. Where possible, the scatter plots of Q versus h resulted in a curve fitting $Q(h)$. For the rivers Don, Ciliwung and Tamar, discharge measurements are infrequent while for the river Ouse, discharge and water level are measured every 15min. The fitted $Q(h)$ are shown in Fig. 2.3a,b,c) and the data in Fig. 2.3d). For the rivers Don, Ciliwung and Tamar, the following type of power-law fit is used for certain river-level stages or intervals

$$Q(h) = c_j(h - a_j)^{b_j} \quad (2.2)$$

with coefficients c_j, a_j, b_j for the j^{th} -stage $h_{j-1} < h < h_j$ with $h_{j-1} > a_j$ and $j = 1, \dots, n_s$ and beyond the last stage/interval, for $h > h_{n_s}$ extrapolation is used. While the unit of a_j is in metres, such that the unit (denoted using the square brackets) $[a_j] = \text{m}$, and b_j is dimensionless, the unit of c_j is $[c_j] = \text{m}^{3-b_j}/\text{s}$. It would make more sense to redefine (2.2) as follows

$$Q(h) = \bar{c}_j(h/a_j - 1)^{b_j} \quad (2.3)$$

with coefficients \bar{c}_j, a_j, b_j such that \bar{c}_j has units of a discharge typical to the j^{th} -stage.

Table 2.1 The 2018 coefficients c_j, a_j, b_j and limb thresholds $h_0 = 0.1890$ and h_j for $j = 1, 2, 3$ for the rating curve of the River Tamar at the river-level gauge station Gunnislake, UK. Courtesy: EA.

j	h_j m	c_j $\text{m}^{3-b_j}/\text{s}$	a_j m	b_j -
1	0.365	30.45	-0.238	3.89
2	3.9840	31.44	-0.00174	2.00

Beyond the highest water and discharge measurements there are no data and the river is in flood so extrapolation tends to be a poor approximation. Sometimes, hydraulic flood simulations are used to create additional rating-curve data. For the River Don at Rotherham Tesco, the EA provided water-level and discharge data and Fig. 2.3a) shows that a smooth rating curve has been used to create smooth discharge data. For the river Ciliwung, there is only one stage such that $Q(h) = c(h - a)^b$ with $c = 11.403\text{m}^{3-b_j}/\text{s}$, $b = 1, 715$, $a = -0.2\text{m}$, see [44], displayed in Fig. 2.3b). Linear approximations to these two rating curves based on the maximum flow rate recorded are shown by the blue dashed slanted lines. For the River Tamar at Gunnislake, coefficients for (2.2) are given in Table 2.1 for a case with two stages/intervals, with rating curve data displayed in Fig. 2.3d). Given that daily data are rather coarse, rating curve data are displayed as individual points $\{Q(h), h\}$. For these three river floods (a,b,d), the intersection of the threshold level h_T with the single-valued rating curve yields one threshold discharge value Q_T as indicated by the dashed thin horizontal and vertical lines. For the River Ouse at Skelton, water level and discharge data are measured in unison every 15 minutes and the situation is seen to be different in Fig. 2.3c). The solid thick data points form a lower branch in the $h(Q)$ -plot when the river is rising and a different upper branch when the river level is sinking. A fourth-order polynomial $Q(h) = a_1h + a_2h^2 + a_3h^3 + a_4h^4$, forced through the origin, is fit through the data and displayed by the dashed curved line. This fit is likely poor and should be ignored outside the region with data for $Q < 180^3/\text{s}$ and $Q > 550^3/\text{s}$. An average threshold value $Q_T = Q(h_T)$ emerges from this fit but the intersections of the horizontal line at $h = h_T$ with the data shows that there are two bounds $Q_{T_{down}}$ and $Q_{T_{up}}$ emerging. In the Ouse case it is therefore not clear whether there is a threshold value of Q , above which there is flooding, in contrast to the other three river-flood cases. Hysteresis, as observed in the Ouse data $h-Q$ plot, often

emerges for river with smaller river slopes, see [33]. The river slopes at the other three flood locations are all larger than the river slope at Skelton in York. Finally, it is a question whether the powerlaw behaviour (2.2) can be based on mathematical analysis of (simplified) hydrodynamic equations, such as the St. Venant equations used in Chapter 4.

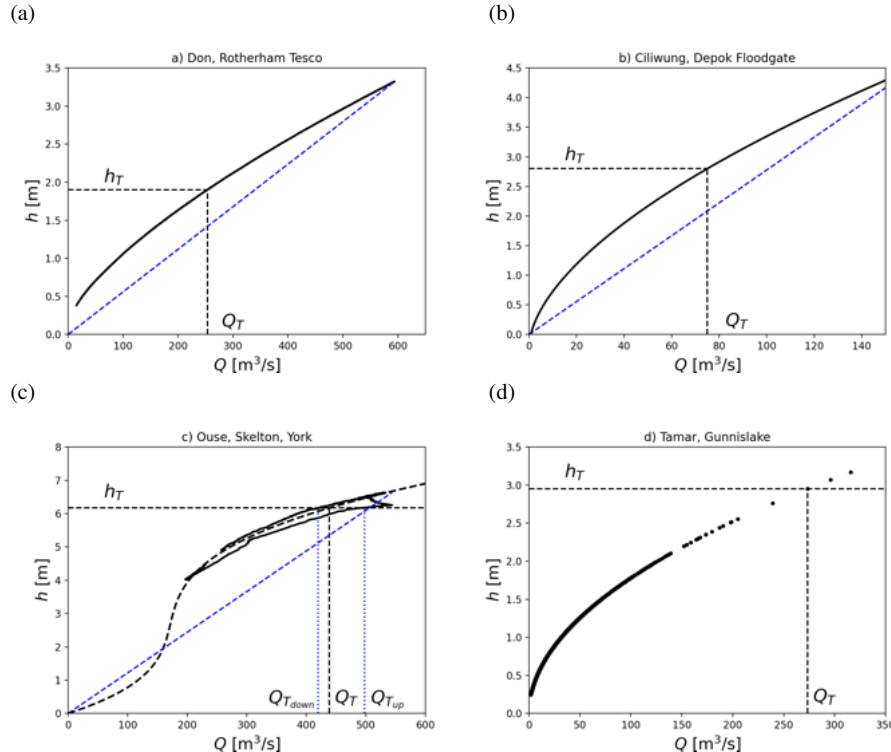


Fig. 2.3 Rating curves $h = h(Q)$ or measurements of water depth h versus discharge Q for: (a) River Don November 08-11-2019 flood at Tesco gauge station, Rotherham, UK; (b) Ciliwung river 01-01-2020 flood at Depok Floodgate gauge station near Djakarta, Indonesia; (c) River Ouse 25-12-2015 flood at Skelton gauge station, York, UK; and, (d) River Tamar 24-12-2013 flood at Gunnislake, UK. Note the nested time dependence $h(t) = h(Q(t))$ or $Q(t) = Q(h(t))$ for the singled-valued rating curves, with a linear approximation indicated by the blue dashed line going through the origin. For the River Ouse both water level and discharge are determined via flow measurements. There are two main rating curves for the River Ouse, one when the river level rises and one when the river level recedes.

2.4 Hydrographs and flood-excess volume

For the four river floods, the hydrographs of discharge $Q(t)$ versus time t are displayed in Fig. 2.4. The discharge data in panels (a,b,d) follow from the water-levels measurements by using rating curves of the form (2.2) while the discharge for the Ouse flood is directly measured. In the latter case, the corresponding h - Q plot was seen to be a scatter plot of the combined water-level and discharge measurements at several times t . Consequently, when there is a single-valued rating curve, each threshold h_T leads to a corresponding and unique discharge threshold Q_T , allowing a straightforward definition of the flood-excess volume.

The flood-excess volume (FEV) is the volume $V_e = V_e(T_f)$ that caused the flooding and, given $Q(t)$ and Q_T , is defined as the volume of the integrated difference $Q(t) - Q_T$ over the duration T_f of the flood, for which this difference is positive. That is, for one identified flood event,

$$V_e = \int_{Q(t) > Q_T} (Q(t) - Q_T) dt, \quad (2.4)$$

which is one interval T_f when there is one peak with $Q(t) > Q_T$ in a flood event or concerns multiple intervals such that $T_f = T_{f_1} + \dots + T_{f_{n_p}}$ when there are several, n_p , local peaks with $Q(t) > Q_T$ in one flood event. When there is one discharge peak Q_{max} with maximum water level height h_{max} , one observes that the FEV goes to zero, such that $V_e \rightarrow 0$, when the maximum discharge and water levels are reached, with $Q_T \rightarrow Q_{max}$ or $h \rightarrow h_{max}$. A straightforward flood defence concerns the building or raising of flood walls or dikes along the river stretch relevant to the chosen river-gauge, thus raising the threshold level $h_T > h_{max}$ for a flood of that magnitude. However, when one raises h_T by introducing flood walls, the discharge patterns and rating curve will also change and one will need to check the extent to which this is the case, potentially via detailed hydraulic simulations. As a first approximation, one can raise h_T while keeping the original rating curve and hydrograph to redefine the FEV.

From the definitions (2.4) of flood-excess volume and flood duration T_f , one can define a mean discharge

$$Q_m = Q_T + V_e/T_f \quad (2.5)$$

and, graphically, an FEV equivalent can also be depicted by a rectangle between Q_m and Q_T over the flooding time T_f .

When one only has the water-level measurements available as well as the maxima h_{max} and Q_{max} , the linear approximation of the rating curve indicated by the straight slanted dashed lines in Fig. 2.3a,b,d) can be employed. Such a linear approximation yields the mean discharge or Q_m -approximations

$$Q_m \approx (h_m/h_{max})Q_{max} \quad \text{and} \quad Q_T \approx (h_T/h_{max})Q_{max}, \quad (2.6)$$

provided one knows the mean water depth h_m during a flood. For idealised rectangular (with peak duration T_f), triangular (with one peak point) or trapezoid (with peak duration $T_f/2$) shape hydrographs (note that for a linear rating curve the shapes of $h(t)$ and $Q(t)$ are the same), the mean water depth can be calculated to be

$$h_m = h_{max}, h_m = \frac{1}{2}(h_{max} + h_T), h_m = \frac{(3h_{max} + h_T)}{4}, \text{ respectively.} \quad (2.7)$$

With (2.6), these lead to the following FEV approximations, see, e.g., [4],

$$V_e \equiv T_f(Q_m - Q_T) \approx V_{e1} \approx T_f(Q_{max} - Q_T), \quad (2.8)$$

$$V_e \approx V_{e2} = \frac{1}{2}T_f \frac{Q_{max}}{h_{max}}(h_{max} - h_T), \quad (2.9)$$

$$V_e \approx V_{e3} = \frac{3}{4}T_f \frac{Q_{max}}{h_{max}}(h_{max} - h_T), \text{ respectively.} \quad (2.10)$$

Such approximations are useful when only Q_{max} is given or when a quick verification is needed.

For the Ouse case, the definition of FEV is ambiguous because there are not only three choices $Q_{T_{up}}$, Q_T , $Q_{T_{down}}$ of threshold discharges but one may also decide to make $Q_T = Q_T(t)$, a function of time t . The three thresholds are indicated in Fig. 2.4 by the horizontal dashed (thicker) blue and (thin) black lines, each line defining a different FEV after integrating the (positive part of the) difference $(Q(t) - Q_{T_{up}})$, $(Q(t) - Q_T)$, $(Q(t) - Q_{T_{down}})$, respectively, for one flood event. Indicated as the red dashed and slanted line is another time-dependent threshold $Q_T(t)$ (notationally distinguished by highlighting this time dependence explicitly), linking the thresholds $Q_{T_{up}}$, $Q_{T_{down}}$ in a linear fashion and yielding another definition of the FEV, as follows

$$V_e = \int_{Q(t) > Q_T(t)} (Q(t) - Q_T(t)) dt. \quad (2.11)$$

One way to resolve these issues is by pursuing detailed hydrodynamic simulations and comparing hydrographs with and without flood-mitigation measures. Another way may be to derive analytical approximations of the river flow that capture some elements of the hysteresis observed, including detailed approximate expressions linking flow and water level.

The FEV is a fraction of the water volume flowing through a river cross-section over the duration of a flood event, during its ramp-up towards flooding and easing to more normal water levels. In addition, during the flood defined as the time T_f for which $h(t) > h_T$ most of the flood waters go through the main channel. FEV is simply defined as the integrated time difference $Q(t) - Q_T$ or, equivalently, the difference between the flood hydrograph and the same hydrograph with a chopped, flat peak at Q_T over the duration T_f of the flood. To obtain a sense of the sizes of rivers in flood, Table 2.2 provides a summary of various floods with FEVs spanning several orders of magnitude from the 2014 Finchingfield flood [20] with $V_e = 0.053\text{Mm}^3$ to

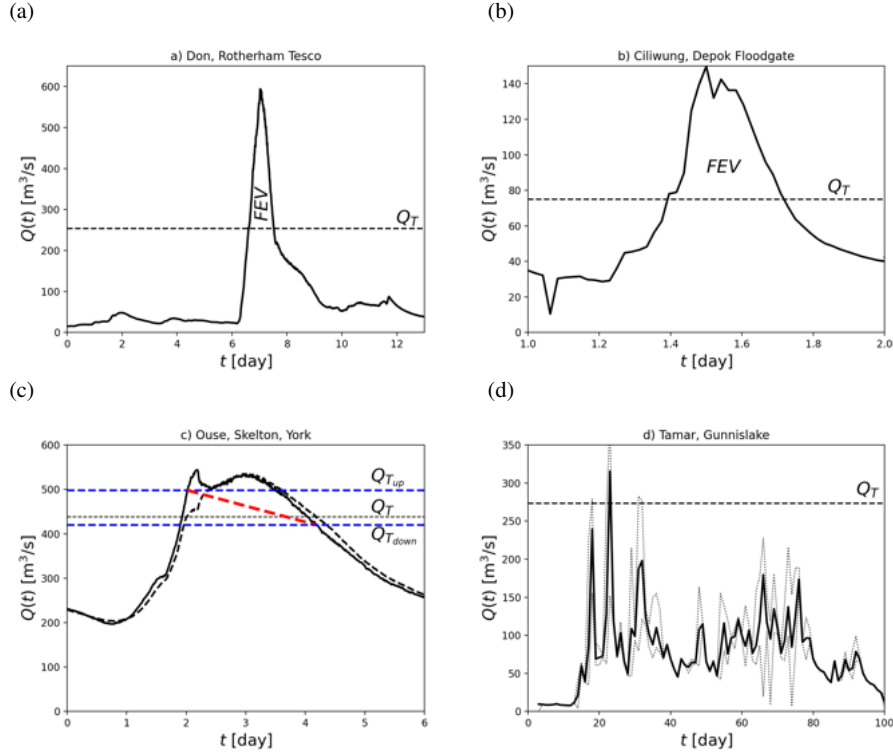


Fig. 2.4 Discharge $Q(t)$ versus time t for: (a) River Don November 08-11-2019 flood at Tesco gauge station, Rotherham, UK; (b) Ciliwung river 01-01-2020 flood at Depok Floodgate gauge station near Djakarta, Indonesia; (c) River Ouse 25-12-2015 flood at Skelton gauge station, York, UK, made every 15min; and, (d) River Tamar 24-12-2013 flood at Gunnislake, UK. The River Ouse has a multi-valued rating curve, essentially one when the river level rises (lower branch in $h-Q$ data) and one when the river levels sinks (upper branch in $h-Q$). For the River Tamar the (daily) minimum and maximum (dashed, thin lines) as well as mean (solid, fat lines) discharges have been displayed.

several floods with $V_e > 3\text{Mm}^3$ and the 2020 Yangtze River flood at Cuntan, China, with an FEV of nearly $V_e \approx 100\text{Mm}^3$, with in particular the 2007/2019 River Don floods in Sheffield and Rotherham as well as the 2015 Rivers Aire and Calder floods causing a lot of damage. Some of the FEVs in Table 2.2 contain error bars, which tend to be rather large, from 16% to over 50%. Calculation of such error bars will be considered in the next chapter. It may, however, still be difficult to attach meaning to the size of floods with FEVs of a million cumecs or more. Consider therefore a flood with $V_e = 2\text{Mm}^3$, divide this FEV by a depth $D = 2\text{m}$ and subsequently take the square root to obtain a side length

$$L_D = \sqrt{V_e/D} = 1000\text{m} \quad (2.12)$$

river -	location -	flood date(s) -	FEV V_e Mm ³	h_T m	L_D m
Aire	Armley/Leeds, UK	26-12-2015	9.34 ± 1.50	3.9	2161
Calder	Mytholmroyd, UK	26-12-2015	1.65 ± 0.60	4.5	908
Don	Sheffield, UK	25/26-06-2007	3.00 ± 0.71	2.9	1225
Don	Rotherham Tesco, UK	08-11-2019	14.2	1.9	2665
Ciliwung	Depok Floodgate, Indonesia	01-01-200	1.05	2.8	725
Ouse	Skelton/York, UK	25-12-2015	$\sim 10.34 (?)$	6.17	2274
Brague	Biot, France	03-10-2015	0.488 ± 0.311	3.06	494
Tamar	Gunnislake, UK	23-12-2012	1.96	2.95	990
Tamar	Gunnislake, UK	24-12-2013	3.65	2.95	1351
Finchingfield Brooke	Finchingfield, UK	07-02-2014	0.053	(?)	163
beaver dam (1 st estimate)	Devon, UK	2015	0.0002	-	10
beaver dam (2 nd estimate)	Devon, UK	2015	0.001	-	22
Yangtze	Cuntan, Chongqing, China	2020	96.25 ± 5	180.5	6973 [†]

Table 2.2 FEVs are given of several river floods with river name, river-gauge location, flood date, FEV (plus error), threshold h_T , and square-lake side length L_D stated. For some floods, error estimates of the FEV are provided as well. FEV estimates for a Devon beaver colony have been added as well, for which h_T is not relevant. For Finchingfield, [20] does not provide a threshold h_T . [†] Provisional data by Shunyu Yao: the error bar is a symmetrised approximate and h , h_T are height above the mean sea level at Wusong near Sjanghai with the river bottom at the Cuntan gauge station lying at circa 174m above sea level.

of a (dynamic) square lake with a two-metres deep human-size depth. The lake is denoted to be dynamic because the FEV generally concerns flowing rather than static flood waters. It can therefore be dubbed a hypothetical or effective lake. If one could find space in the river valley upstream of the flooded region of interest, to store extra flood waters in a lake of that size or in an accumulation of smaller lakes with that total size, then the flood could likely be annulled or mitigated. Given the size of such a square lake of a flood, it can be compared with the dimensions of potential storage sites in the river valley. If the river valley is narrow and/or build-up, then finding such storage sites may be a task that is difficult to achieve. The (dynamic) lake side-lengths L_D for each flood are found in Table 2.2 as well and are seen to range from 163m to 2665m and even ~ 7000 m for the 2020 Yangtze flood at Cuntan.

2.5 Storage-based protection measures

Both the (critical) water levels h_T and h_{max} as well as the FEV, V_e , for a particular flood classify its magnitude. To protect against flood damage of floods with a similar magnitude, people may wish or decide to reduce the FEV to zero and possibly also partially raise h_T by introducing a variety of flood-mitigation measures. When FEV is used, the focus will lie on effective storage-based measures, or their equivalent, reducing the in-situ h_{max} , while when $h_T \rightarrow h_{max}$ focus lies on reaching the peak

water-level value with flood defences. Both approaches are valuable. Focus here will be placed on storage-based methods since the use of the chosen threshold h_T includes the limiting of $h_{max} \leq h_T$. Also recall that the discussion on building or raising flood-defence walls is seen to translate into $Q_T(t) \rightarrow Q_{max}$ such that the FEV reduces to zero, $V_e \rightarrow 0$, given that $h_T \rightarrow h_{max}$. One caveat in using the FEV (or threshold h_T) of a particular flood, using either measured or simulate data is that the FEV generally changes a (little) bit when one introduces flood-mitigation measures because these measures will affect the river-bed and flood-plain characteristics. When the FEV is kept unchanged in discussing and quantifying flood-mitigation measures, one has to keep in mind this caveat, which can be overcome by detailed simulations or approximated calculations that include changes in those characteristics. A brief, pictorial overview of storage-based flood-mitigation measures will be provided next.

Flood-defence walls: Heightening flood-defence walls or berms/dikes (HW) leads to a reduction of the FEV by increasing h_T and, hence, $Q_T(t)$, see Fig. 2.5a,b). More simply put: (dynamic) water volume is “stored” between the walls when these are raised.

GRR: Giving-room-to-the-river (GRR) concerns a series of interventions which increase the conveyance of the river bed and flood plains. GRR can include lowering and widening river banks, as well as opening up old or creating new river branches to allow more flow and storage in floods, see Figs. 2.5c and 2.6d).

Flood-plain storage: Flood-plain storage (FPS) can be achieved in various ways: by lowering summer dikes such that the river overflows onto the adjacent flood plains more easily (e.g., also called washlands) or by constricting the river banks with dikes or berms on the flood plain such that more flood waters are stowed onto the flood plain upstream of such a constriction. Such constrictions can be made via static berms upstream of fixed weirs or dynamically by using berms and dikes on the flood plain with a moveable, i.e. controllable, weir in the river. Dynamic or active control of the weir can then be used to optimize flood-water storage on the adjacent flood plains. In both these passive and active cases, extra water volume is stored onto the flood plains and in the river relative to the flood situation without these interventions, see Fig. 2.5e).

Natural Flood Management: Natural flood management (NFM) is a broad category involving various options, such as a multitude of leaky dams built from natural materials, or tree planting to retain more precipitation/water, generally in the natural upstream portions of a river catchment, see Fig. 2.5f) and Fig. 2.7g). Each leaky dam by itself is an example of (the use of a passive weir constructed by using natural materials in) FPS but given that the storage volume per leaky dam tends to be small relative to the required FEV, the accumulation of FPS behind an accumulation of such leaky dams in an area, placed in series on a tributary or in parallel over several tributaries connected to a main channel, is categorised as NFM [18].

Beaver dams: Beaver colonies and dams (BD), essentially a form of NFM, are thought by some people to create and deliver flood protection since their dams are thought to hold a sufficient amount of flood waters [40, 35, 26], see Fig. 2.7h). Such beaver dams are a particularisation of the leaky dams mentioned under NFM.

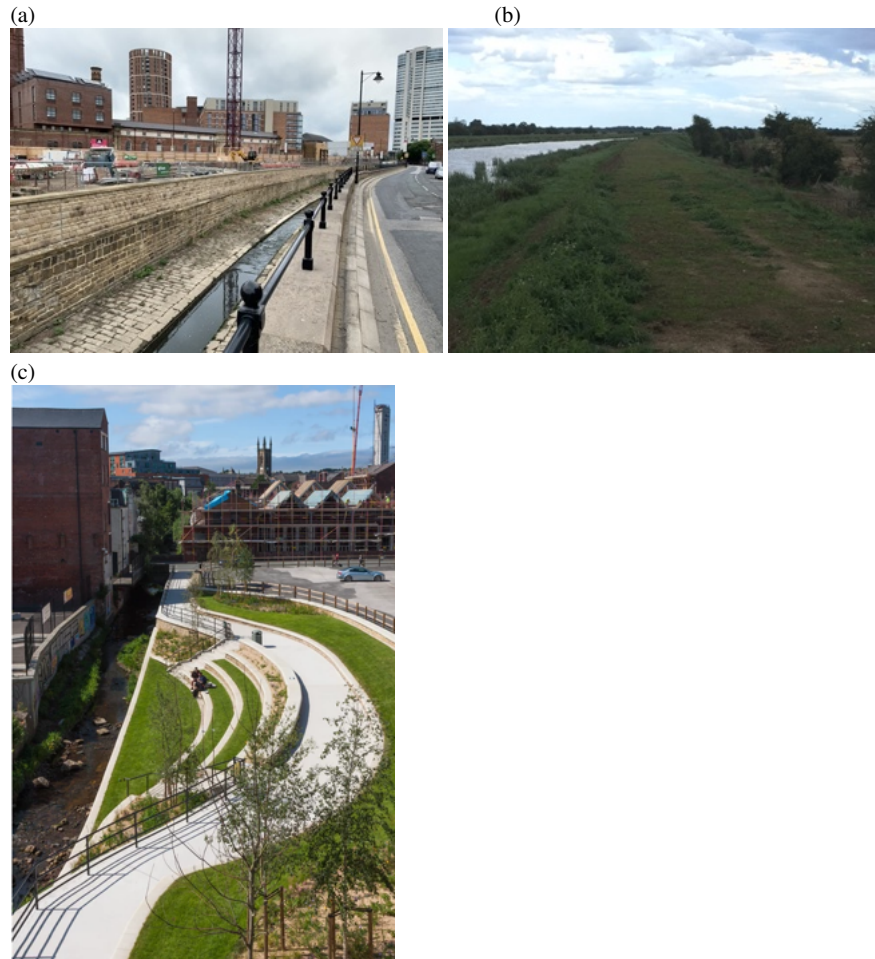


Fig. 2.5 Storage-based flood-mitigation measures (a) flood-defence walls (HW) along the Holbeck near the River Aire in the centre of Leeds have been raised after the 2015 Boxing Day Floods; (b) a heightened and repaired berm or dike (HW) along the relief canal north of Wainfleet, Lincolnshire, UK, after the berm breached in June 2019, flooding parts of Wainfleet and the surrounding area; (c) river-bank lowering and widening (GRR) in the form of the multi-use Porter Brooke Pocket Park along the River Sheaf in Sheffield, UK, established in response to the 2007 floods in Sheffield; Courtesy: photo of Porter Park by Sheffield Society of Architects. [Placeholders photo for c\); alternative River Dinkel in NL available or travel to Sheffield to take photo.](#)

(d)



Fig. 2.6 Storage-based flood-mitigation measures (d) a new alleviation channel or cut (GRR) for the River De Waal (the largest tributary of the River Rhine) at Nijmegen, The Netherlands; the main river is seen on the left and an old river branch on the right has been reopened and deepened as alleviation channel during high water levels and as recreational space during normal and low water levels. A similar alleviation channel is found at Kirkstall The Forge in the River Aire upstream part of Leeds. It is a new cut made after the 2015 Boxing Day floods, which is dry during normal conditions but tempers the water-level increase in part caused by the sharp bend in the river during flood conditions, thus keeping the railway tracks dry longer. Courtesy: 2015 photo of River De Waal by Wout Zweers.

Nature-based Solutions: Nature-based Solutions (NBS) are a broad category concerning flood-mitigation measures inspired by natural aspects. NFM and beaver dams are consequently included but NBS is a broader category and can include green and hybrid grey-green engineering solutions. Some GRR measures can sometimes also be dubbed as NBS.

2.6 Available flood-storage volume

The storage-based flood-mitigation measures discussed above can be quantified by using the concept of available flood-storage volume [4]. Available flood-storage volume is the volume available above and beyond the storage capacity of the river and its floodplains already occupied by a flood of a certain magnitude. It is important to realise that it is an effective and generally dynamic storage volume, since the river water will in most cases be flowing through but possibly at a lower speed. Regarding the quantification of new measures, available flood-storage volume can alternatively be defined as the difference between the total storage volume for a certain flood-

(e)



(f)



(g)



(h)



Fig. 2.7 Continued. (e) flood-plain storage (FPS) on washlands of the River Aire with its summer dikes visible during Storm Ciara 09-02-2020 floods; (f) sketch of dynamic FPS with a moveable weir; (g) leaky dam (NFM) made of logs over the Sutherland Beck in North Yorkshire (guided tour to a beaver colony in North Yorkshire on 12-03-2020); (h) beaver dam (BD) across the the Sutherland Beck in North Yorkshire. Courtesy images: e) Robin Attrill (aerial) and f) sketch by Leeds City Council. Placeholder photos for e,f). Alternatives under consideration.

mitigation measure and the existing total storage volume in a certain area prior to implementation of that measure for an event of the same magnitude. For example, if the flood-plain providing storage volume $A_p d_p$ upstream of a contraction in the river, natural or otherwise, involved a flood depth $d_p = 3\text{m}$ on average over an area A_p , and if extra flood storage would be achieved by further (partial) blocking of the contraction leading to an average water depth of $d_e = 4.5\text{m}$ over an area $A_e \geq A_p$, with a total storage volume of $A_e d_e$, then the available flood-storage volume would be the difference $A_e d_e - A_p d_p > A_p 1.5\text{m}$. For a flood of lower magnitude the average depth d_p and area A_p will be smaller and there would potentially be more available flood-storage volume achievable if the maximum $d_e = 4.5\text{m}$ can still be reached, for example by further reduction of the contraction area in a controllable fashion.

The manner in which the contraction is controlled or controls itself via its fluid dynamics does matter, as the following example illustrates. If prior to the arrival of the water-level increase during a flood event or prior to the flood peak the flood-storage area is already (partially) filled above $d_p > 3\text{m}$ and possibly even filled fully to level of $d_e = 4.5\text{m}$ then there is less or no flood-storage capacity left and the available flood-storage volume is suboptimal or even zero. Using the maximum available flood-storage volume therefore becomes a control problem when active control of the contraction area is available, for example by opening or closing the dynamic weir in a prescribed manner [10, 11, 47]. The concept of available flood-storage volume will be explored in two examples in the next two sections, one involving beavers as natural engineers creating storage ponds behind their beavers dams and one concerning control, either optimised by humans or beavers, each with their own cost function.

2.7 Upscaling flood-water storage behind beaver dams unrealistic?

In both scientific literature [40, 26, 35] and the (British) media, water storage via colonialisation of a river valley by beavers has been proposed as a (potential) flood-mitigation measure to reduce floods. To assess that potential it is necessary to look at available measurements of the hydrology and hydrodynamics of beavers colonies and the particular effects of their beaver ponds and dams. The change in time of the storage volume V_b of a beaver pond or a series of beaver ponds depends on the influx Q_{in} , outflux Q_{out} and evaporation E_v (all expressed as rates). Cf. the analysis in [26] we find

$$\frac{dV_b}{dt} = Q_{in} - E_v - Q_{out}, \quad (2.13)$$

in which Q_{out} can be divided further into outflow from the dam Q_{dam} , groundwater outflow Q_{gw} and return flow Q_{rf} from the floodplain downstream of the dam such that $Q_{out} = Q_{dam} + Q_{gw} + Q_{rf}$. Measurements of the inflow Q_{in} and (part of)

the Q_{out} will be shown for beaver-dam complexes in the River Tamar catchment in Devon, UK [40], along the Chevral River in the Ardennes, Belgium [35], and in streams crossing coastal wetland in Northern Ontario, Canada [48].

Two hydrographs are shown in Fig. 2.8 at a weir of the river flow upstream of a series of 13 beaver dams and ponds over a length of circa 200m in Devon and at a weir downstream of this beaver colony for a flood peak around 12-12-2014. Puttock et al. [40] investigated a series of such flood peaks, the in- and outflows, and report a storage volume of circa $V_b = 1100\text{m}^3$ (here taking a convenient limit above the mean but within the reported error range). In addition, they conclude that “*beavers are likely to have a significant flow attenuation impact*” and “*to develop and understanding how beavers may form a ‘nature based solution’ to . . . flooding problems faced by society*”. Given this storage volume V_b and the FEVs of several river floods, as found Table 2.2, it follows how many beaver colonies of the Devon-type are required to mitigate 1%, 10% or 100% of the FEV, where in the first two cases 99% or 90% of the relevant FEV preferably ought to be covered by other mitigation measures to provide full protection against floods of the chosen magnitude. The number of beaver colonies of the Devon-type, in the optimal case of the full storage being used and without any dam collapse, is then

$$(0.01, 0.1, 1)V_e/V_b, \quad (2.14)$$

respectively, for (1, 10, 100)% coverage. For the various river floods, that number of required beaver colonies lies between 48 and 9400 (and 5 to 940 colonies for 10% coverage). E.g. 48 beaver colonies would be required to reach 100% coverage of the FEV for the smallest flood in the table, the Finchingfield flood. For a flood with $V_e = 1.1\text{Mm}^3$, one would need (10, 100, 1000) beaver colonies to achieve (1, 10, 100)% coverage, involving (130, 1300, 13000) beaver dams (13 beaver dams per colony) and (40, 400, 4000) beavers (using four beavers per colony) over a length of (2, 20, 200)km distributed over the relevant river catchment (using 200m per colony). Table 2.3 provides a summary of some of these numbers. Hence, such large numbers of beaver colonies required reveal that there seems to be no potential for serious flood mitigation by using beavers, even for the smaller fractions of FEV-coverage by the available flood-storage volume of beaver ponds.

Further understanding of that lack of potential is obtained by addressing the following questions:

- is the value of V_b used from the Devon beaver colony representative, and
- is the ratio (V_b/V_e) of available flood-storage storage volume (V_b) for a particular mitigation measure over the required FEV (V_e) providing an adequate estimate to assess the effectiveness of a flood-mitigation measure?

The second question will be considered in chapter ???. The first question is analysed in several ways, next:

- The available flood-storage volume for a beaver-dam complex can either be found from two hydrographs, one taken before the beavers started building their dams and one thereafter during a heavy rainfall flooding period, or from one hydro-

graph taken prior to a heavy rainfall and flooding period and during this period. Alternatively, the available flood-storage volume can be estimated by obtaining the average pond-level fluctuations times the pond area. Such area estimates can follow from aerial photographs. Estimates in the uncertainty of that volume can be estimated by considering beaver-dam complexes in different areas, in different landscapes and over time.

- The flood-storage volume over a unit river length can be estimated by taking into account a (hypothetical) density of beaver colonies along a main river and its tributaries.
- Given the FEV of a target or design flood, the above allows one to calculate how many beaver colonies would be needed to cover a certain fraction of the FEV. Additionally, the density estimates permit one to assess whether there is sufficient space in a river catchment for (an abundance of) beaver dams.

One caveat arises in that the scientific literature on beavers with adequate flood hydrographs appears to be limited, thereby restricting the following analysis.

The appropriateness of the value of $V_b \approx 1100\text{m}^3$ is, furthermore, straightforward to check from one of Puttock et al.'s hydrographs, adapted in Fig. 2.8, showing a roughly estimated volume of circa 900m^3 . There is, however, a caveat in the above analysis, reported by [39]. The surface area of the beaver ponds is said to be circa $A_s = 2000\text{m}^2$, which also follows by estimation via [40]'s Fig. 2 (top left) as circa $A_s \approx 25\text{m} \times 100\text{m} = 2500\text{m}^2$ (i.e., the valley width times accumulative length of the beaver ponds is the area covered by beaver ponds). The depth increase Δh in a flood event is seen to be small in Puttock et al.'s Fig. 2 (bottom [40]), circa 0.1m on average except for a few events for one pond, where $\Delta h \approx 0.5$ to 0.8m. These adapted estimates yield an available flood-storage volume of $V_b = A_s \Delta h \approx 200\text{m}^3$ which is circa a fifth of the reported value of $V_b \approx 1100\text{m}^3$. The origin of this difference is unclear: there may be evaporation losses E_v , unaccounted for groundwater and return flows Q_{gw} , Q_{rf} , and/or the hydrograph measurements may contain larger errors than reported. In the next chapter, errors of various FEVs will be estimated to lie in the range of 15% to over 50%. In addition, for this event inspection of Fig. 3 in [40] shows that water volume may be missing since Q_{out} is not larger than Q_{in} after the peak event to account for the stored volume being released at later times.

The next beaver site considered is located on flat wetlands near Hudson Bay in Northern Ontario, Canada [48]. This region is extremely flat and numerous beaver ponds have been observed; Woo and Waddington [48] mention 60 beaver dams in various states of preservation in a 1km^2 area. Given its close proximity to the coast, their estimates of storage volume may be less relevant to river-flood cases considered in Table 2.2, so the resulting outcome should perhaps be taken as an upper limit. Dam density ranges from 5 to 19dams/km, with an average of 14.3dams/km. Woo and Waddington [48] note that this density is close to the 10.6dams/km in South-eastern Quebec but higher than the 2.5dams/km in Northern Minnesota [34]. The discharge reduction due to one beaver dam near Ekwan Point, North Ontario, can be calculated from the difference of the inflow hydrograph and the outflow hydrograph during a rainfall event on 21-06-1988, see Fig. 8 of [48]. Approximate integration by drawing in a rectangle of equivalent area to the actual area between the two hydrographs

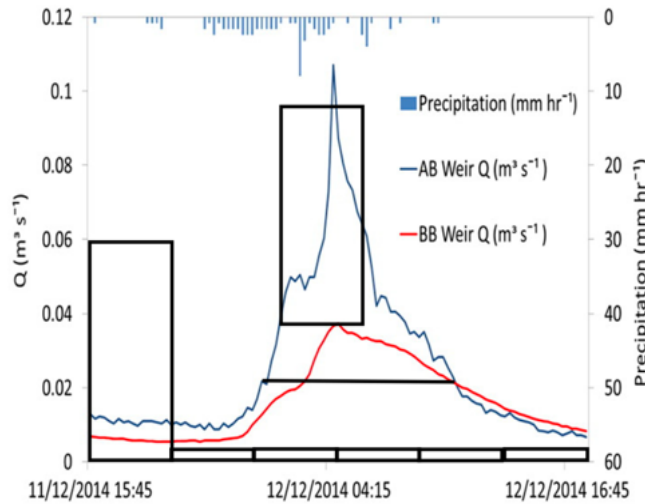


Fig. 2.8 Hydrographs at weirs upstream (AB, blue line) and downstream (BB, red line) of a beaver colony for a flood peak in a tributary of the River Tamar, in Devon, UK. Taken and adapted Fig. 3 (bottom-left) from [40] with the approximate (eye-ball) integration technique displayed. The rectangular box drawn in is roughly equivalent to the desired area of integration between the two hydrographs of the flood peak. Measurements of that rectangle ($0.06\text{ m}^3/\text{s}$ over $23/6\text{hr}$) along the respective axes indicate that it concerns rectangle sides of $\sim 0.06 \times (25/6) \times 60 \times 60\text{m}^3 = 900\text{m}^3$. Note that more precision is not required for obtaining an estimate.

around the peak flow, i.e. by using eyeball measures and subsequent estimates of the rectangle's sides, yields an effective storage volume of $V_b = (10/6.33) \times 24 \times 3600 \times 2 \times 10/7\text{m}^3 = 390\text{m}^3$ behind one dam, cf. Fig. 2.9. Whether there are significant other losses such as evaporation for this site is unknown. In addition, error estimates on the hydrographs are unknown and [48] seems to contain insufficient information to check the volume V_b as the multiplication of the pond areas times the height difference, i.e. as $A_s\Delta h$, although the authors state that they have used such estimates. Given the dam density, we have a high storage per kilometre of river network, i.e.

$$V_{Ek} = 14.3 \times 390\text{m}^3/\text{km} = 5570\text{m}^3/\text{km}. \quad (2.15)$$

There may be water fluxes missing, since the measured outflow does not seem to be sufficiently larger than the inflow after the flood event upon inspection of the two hydrographs in Fig. 2.9 to account for the total mass balance. Evaporation losses could, however, be large and account for the difference.

Combining [42]'s reported colony density between 3km and 20km with [40], a dam density estimate for the Devon case lies between $(13/20)\text{dams/km} = 0.65\text{dams/km}$ and $(13/3)\text{dams/km} = 4.33\text{dams/km}$. Given that there are 13 dams in Devon with a quoted effective volume of 1100m^3 , the volume stored per dam is $(1100/13)\text{m}^3/\text{dam} = 85\text{m}^3/\text{dam}$. Hence, by taking the best case, the storage volume

per kilometre in the Devon case becomes

$$V_{De} = 85 \times 4.33 \text{m}^3/\text{km} = 367 \text{m}^3/\text{km}, \quad (2.16)$$

an order of magnitude less than estimate (2.15) in the Ekwon Point case. Given that [39] argues that the 1100m^3 is a factor five too large, a second estimate becomes $V_{De2} \approx 75\text{m}^3/\text{km}$.

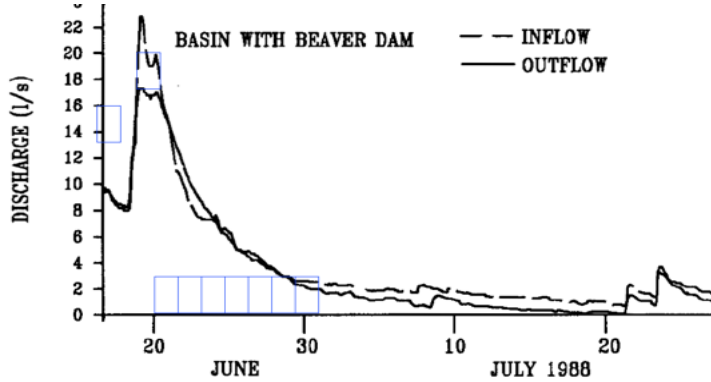


Fig. 2.9 Taken and adapted Fig. 8 from [48] with integration techniques displayed. The rectangular box drawn in is roughly equivalent to the desired area of integration between the two hydrographs of the flood peak. Measurements of that rectangle along the respective axes indicate that it concerns rectangle sides of $\sim (10/6.33)\text{days}$ and $\sim 2 \times (10/7)\text{l/s}$ yielding $V_b = 390\text{m}^3$. Again note that more precision is not required for obtaining an estimate.

The review article [26] includes two hydrographs around 28-02-2010 with Q_{in} and (part of) Q_{out} from [35], shown and adapted here in Fig. 2.10, concerning a beaver colony along the Chevral River in the Ardennes in Belgium. What is immediately clear is that the storage volume $V_b = 1.782\text{Mm}^3$ is not released later in the Q_{out} hydrograph, so there is water volume missing, either due to evaporation, groundwater flow or floodplain flow around the point of outflow measurement? As independent estimate, one observes that there are six beaver dams over a river stretch of 300m. Using Figs. 3 (taken at lower water levels than the peak on 28-02-2010) and 6 of [35], a generous estimate yields a water-covered area of $A_s = 300 \times 50\text{m}^2 = 15000\text{m}^2$ and by taking a generous pond-height difference $\Delta h = 2\text{m}$, a volume estimate of $V_B = A_s \Delta h = 30000\text{m}^3$ results, far off the difference between the two hydrographs. To be clear, the authors indicate “extrapolations beyond range of observation”. In their Table 4, the volume stored in the pond relative to that stored at 30-09-2009 is stated but those volumes do not seem to be the relevant available flood storage volumes. Given this spread in possible values of V_b and lack of clarity on the values for V_b , the results from [35] are discarded. In general, there is plenty of literature on beaver colonies with remarks on beaver ponds holding flood waters but it seems

much more difficult to find data verifying or defining what the relevant available flood storage volumes are.

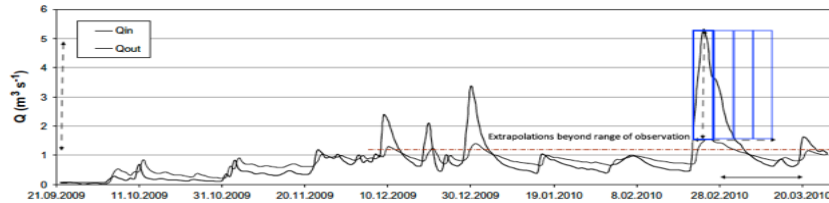


Fig. 2.10 Taken and adapted Fig. 12 from [35] with integration techniques displayed. The rectangular box drawn in is roughly equivalent to the desired area of integration between the two hydrographs of the flood peak. Measurements of that rectangle along the respective axes indicate that it concerns rectangle sides of $\sim (20/4) \times 24 \times 3600\text{hr}$ and $\sim 4\text{m}^3/\text{s}$ yielding $V_b = 1.728\text{Mm}^3$.

Chaubey and Ward [12] report hydrographs of inflow and outflow for two storm events in 1994 in Talladega Wetland, West Central Alabama, USA, one is consistent in showing that the outflow picks up after the event, releasing a volume similar in size to the estimated storage volume of $V_b = 3600\text{m}^3$ with a lowered outflow peak delayed by about 3 to 4 hours, and another one which shows the outflow exceeding the inflow due to overflow of the beaver dam and a record in time displayed that is too short to assess consistency. There seem to be about five beaver dams over a length of 200m so the storage per beaver dam would be about 600m^3 and with the highest density of 4.33dam/km , the storage per kilometre then becomes

$$V_{Tal} = 2598\text{m}^3/\text{km}. \quad (2.17)$$

This latter value is consistent with V_{Ek} , which larger value is used hereafter.

Given these three beaver-pond available flood-storage densities V_{Ek}, V_{De}, V_{De2} , a triplet range

$$R_{100} = [V_e/V_{Ek}, V_e/V_{De}, V_e/V_{De2}] \quad (2.18)$$

can be defined, yielding the hypothetical range of lengths for the respective river networks to mitigate the FEV for 100% under ideal circumstances. These lengths, as well as a tenth thereof, are compared with main river lengths in Table 2.3. It shows that using beavers as flood-mitigation strategy appears to be unrealistic. These lengths needed within one river catchment, including its tributaries, are too large despite all the favourable assumptions used. The analysis above shows that the estimates are surrounded by a lot of uncertainty. Other assumptions used are that the beaver dams are perfect, do not collapse and are all used to full capacity. Dams arranged in series could cause an accumulation of collapsing dam and debris flows during extreme floods. The analysis does show how the efficacy of a certain measure proposed, here beaver dams, can be readily assessed using FEV and hydrograph analysis. Finally, both the lead author of [39] and I are in favour of reintroducing more beavers in

the wild and are, furthermore, arguing in a quantifiable manner that there is both no need and no justification to promote beavers as actors in flood mitigation in order to justify this otherwise just cause of wildlife enhancement.

Finally, Piton in [39] suggests that beavers may have a different objective than flood mitigation: the beavers' goal is to minimise fluctuations in beaver ponds such that their beaver burrows are neither subject to pond-level decrease in droughts nor to pond-level flooding in floods. Beaver burrows, see for example Fig. 2.11, have an entrance under water to a drying chamber and a dry top chamber. The beaver's objective may possibly be to keep the entrance under water, to deter intruders, and keep both chambers dry, which requires the pond's water level to stay between two limits. Such different objectives by humans and beavers will be explored mathematically by exploring two different cost functions in the next section. The model will involve a porous dam which porosity can be varied and used as control in attempts to reach the respective objectives.

River -	flood date(s)	length km	V_e Mm ³	R_{100} km	0.1 R_{100} km
Aire	26-12-2015	148	9.34 ± 1.50	[838,12725,62333]	[168,2545,12640]
Calder	26-12-2015	72	1.65 ± 0.60	[296,4496,22000]	[296,4496,2200]
Don	25/26-06-2007	142	3.00 ± 0.71	[539,8174,40000]	[54,817,4000]
Tamar	23-12-2012	98	1.96	[352,5341,26133]	[35,534,2613]
Tamar	24-12-2013	98	3.65	[655,9946,48667]	[66,995,4867]
Finchingfield	2014	~ 11 (?)	0.053	[10,144,707]	[1,14,70]

Table 2.3 Given $V_{Ek} = 5570\text{m}^3/\text{km}$, $V_{De} = 367\text{m}^3/\text{km}$ and $V_{De2} = 75\text{m}^3/\text{km}$, a range $R_{100} = [V_e/V_{Ek}, V_e/V_{De}, V_e/V_{De2}]$ is defined, yielding the hypothetical range of lengths of the respective river networks to mitigate the FEV for 100% under ideal circumstances. In addition, 10% of these lengths, in the column indicated by $0.1R_{100}$, are calculated assuming that the remaining (fraction of the) FEV is either left unmitigated or is mitigated by other flood-mitigation measures. We have also given river lengths but note that Leeds, Mytholmroyd, Sheffield are lying in the upper half or third of the respective rivers, while Gunnislake is at the end of the non-tidal part of the River Tamar in which the Tamar catchment is the one with the Devon beaver colony [40]. FEVs concern floods in the cities or villages mentioned. The given cumulative length of the brooks upstream of the village of Finchingfield is a rough estimate based on inspection of a map; hence, the question mark.

2.8 Controlling water levels: human versus beaver engineering

To do using porous dam formulation in [18] but with controllable porosity; using smart flood control on the discharge Q , making matters linear for Q , except for the a posteriori relation to porosity and water level, cf. Willemsen et al. - Explore hypotheses. - Two cost functions for hydraulic control (human and beaver one). - Some exact maths and hydraulics examples using HESS article of Study Group



Fig. 2.11 Beaver burrow in Sutherland Beck, North Yorkshire, UK, on the bank of the beck with an underwater entrance –guided tour to a beaver colony in North Yorkshire on 12-03-2020.

that can be modified into mini-control problems. - Phrase in terms of available flood-storage volume with some mathematics. (All new. Incompleted start below.)

Consider a porous dam of height H with (one-dimensional) porosity ϕ such that ϕH is the accumulative length of holes in the dam. A straightforward model will be formulated of approximate hydraulic river flow upstream of a porous dam and downstream of a porous dam. The slope S of the river is taken constant. The model is inspired by the model with routed and branched flow between nodes as used in [18]. Here, only one such branch will be considered between an upstream and downstream node, with a village lying at the node downstream of the dam. A sketch of the situation is provided in Fig. ???. Subsequently, the fate of the river flow in the village under extreme rainfall and extreme drought upstream of the dam will be considered for two optimisation cases; a time-dependent porosity parameter $\phi = \phi(t)$ will be used, as follows: (i) by humans in an attempt to keep the flow depth in the village below a flood threshold level, and (ii) by beavers in an attempt to keep their beaver burrow in the lake upstream of the dam both dry in flooding and the burrow entrance submerged under droughts.

Appendix

River flow upstream and downstream of a porous dam

Consider river flow in an upstream reach and a downstream reach of a porous dam. The porosity of the dam can be manipulated within certain bounds such that the flow through the dam can be optimised to keep the habitat of either humans in a village downstream of the dam or beavers in their burrow within the dam pond inhabitable. The optimisation goal of the humans is to keep the river level $h_{city}(t) < h_{threshold}$ at a critical location in the city below a certain threshold $h_{threshold}$, such that (major) flooding is avoided during (extreme) rainfall. The optimisation goal of the beaver family is to keep the pond level $h_{pond}(t)$ at the beaver burrow upstream of the dam bounded: $h_{min} < h_{pond}(t) < h_{max}$. Beaver burrows have an entrance under water as protection against predators with a lower chamber to dry out and a dry upper chamber. These chambers should preferably stay dry during floods and the burrow's entrance should stay submerged during droughts.

A simplified hydraulic model will be developed next to be used in optimisation procedures. The goal is to assess the successes and failures of such optimisation under some representative rainfall scenarios. The upstream river reach has constant length l_1 , mean cross-sectional area $A_1 = A_1(t)$, the inflow from rainfall flowing into this upstream reach is given by volumetric source $q_1 = q_1(t)$ and the volumetric outflow by $Q_1 = Q_1(h_1)$. The downstream river reach has constant length l_2 , inflow Q_1 from the upstream reach and outflow Q_2 and mean cross-sectional area $A_2 = A_2(t)$. In reach-2, the river channel is uniform and as first approximation rectangular in cross-section with mean width w_r and mean depth $h_2(t)$. Its downgradient river slope is S_2 and the specified rain drainage $q_2 = q_2(t)$. The outflow Q_2 is approximated using Manning's balance between a quadratic turbulent frictional parameterisation and the downgradient component of the force of gravity [?, ?], yielding a mean flow in the reach set equal to the outflow

$$Q_2 = \frac{S_2^{1/2}}{n} = \frac{(w_r h_2)^{5/3} S_2^{1/2}}{(w_r + 2h_2)^{2/3} n}, \quad (2.19)$$

wherein $A_2 = w_r h_2$ is the cross-section area of reach-2, $R_2 = w_r + 2h_2$ the wetted perimeter and n the Manning coefficient, for the rectangular river channel.

The flux at the porous dam depends on the water level h_1 immediately upstream of the dam, which has fixed height H . First, consider an underflow gate of a weir of height H and a bottom gap of height $a \ll h_1$. With an upstream velocity $V_1 \ll gh_1$ and downstream velocity V_2 , the shallow-flow balance is $V_1^2/2 + gh_1 \approx gh_1 = V_2^2/2 + gh_2 \approx V_2^2/2$ such that $V_2 = \sqrt{2gh_1}$. The flow rate through the bottom gate is then ([?], pp 460) $Q_1 = C_d a V_2 = C_d a \sqrt{2gh_1}$ with empirical contraction coefficient $C_d \in [0.45, 0.6]$. The water level downstream of the dam is taken to be the mean water level h_2 of reach-2. When $h_1 < H$ the flux through the porous dam is similarly taken to be [18]

$$Q_1 = kh_1 \sqrt{2gh_1} \quad (2.20)$$

with kh_1 akin to the effective “gap” width times contraction coefficient $C_d a$ and k the dam permeability, including both the porosity and contraction effects combined. When the level $h_1 > H$, water will be spilling in a jet over the dam. This spilling overflow is ([?], pp 455)

$$hallo \quad (2.21)$$

and combined with (2.20) evaluated at the dam top H , the total outflux for both situations then reads

$$Q_1 = \begin{cases} h \\ \end{cases} \quad (2.22)$$

For the rectangular river cross-section

$$A_2 = w_r h_2. \quad (2.23)$$

In reach-1, the flow upstream of the dam pond is again approximated using Manning’s approximation, as in (2.19), yielding

$$\hat{Q}_1 = \frac{S_1^{1/2}}{n} = \frac{(w_1 \tilde{h}_1)^{5/3} S_1^{1/2}}{(w_1 + 2\tilde{h}_1)^{2/3} n}, \quad (2.24)$$

with constant river level $\tilde{h}_1 \ll h_1$. It has cross-section $w_1 \tilde{h}_1$ for a rectangular section. When we consider a flat pond level, the pond has triangular shape and, given reach slope S_1 extends $(h_1 - \tilde{h}_1)/S_1$ along the river reach and the mean pond depth is $(h_1 - \hat{h}_1)/2$. The mean cross-section is then the weighted average

$$A_1 = \frac{1}{2} w_1 (h_1 - \hat{h}_1)^2 / (S_1 l_1) + (h_1 - \hat{h}_1) \hat{h}_1 / (S_1 l_1) \quad (2.25)$$

$$\implies \hat{h}_1 = \sqrt{\cdot}. \quad (2.26)$$

Given the above considerations, the mass balance in both reaches is then approximately as follows

$$l_1 \frac{dA_1}{dt} = q_1 - Q_1 \quad (2.27)$$

$$l_2 \frac{dA_2}{dt} = q_2 + Q_1 - Q_2 \quad (2.28)$$

Pontryagin’s Maximum Principle:

$$J = \int_{t_0}^{t_1} f_0(x_1, x_2, u) dt \quad (2.29)$$

$$H = \psi_0 f_0(x_1, x_2, u) + \psi_1 f_1(x_1, x_2, u) + \psi_2 f_2(x_1, x_2, u) \quad (2.30)$$

$$\dot{\psi}_i = -\frac{\partial H}{\partial x_i}, \quad i = 0, 1, 2 \quad (2.31)$$

to-be-minimised function, Hamiltonian and adjoint equations.

Let $u^*(t)$ admissible control, corresponding path \mathbf{x}^* transfers system from \mathbf{x}^0 at $t = t_0$ to \mathbf{x}^1 at some unspecified $t = t_1$. In order that u^* , \mathbf{x}^* be optimal and J minimised there exist a nontrivial vector $\psi = (\psi_0, \psi_1, \psi_2)$ satisfying the adjoint equation and with a scale Hamiltonian H such that

- for every $t_0 \leq t \leq t_1$ Hamiltonian H attains its maximum with respect to u at u^* ; and,
- $H(\psi^*, x^*, u^*) = 0$ for $\psi_0 \leq 0$ at $t = t_1$ with ψ^* solution at u^* . Furthermore, H is constant such that $H = 0$ and $\psi_0 \leq 0$ at each point on an optimal trajectory.

Chapter 3

On communicating flood-mitigation plans

Abstract A graphical cost-effectiveness tool to design, assess and communicate flood-mitigation plans is introduced. It is on purpose straightforward such that it is comprehensible to stakeholders in the decision-making process of flood mitigation plans, with these stakeholders including the interested and affected general public. The basis of the tool lies in the usage of the flood-excess volume (FEV) of a particular chosen flood event at a particular critical location. The tool links the magnitude or effectiveness of each proposed mitigation measure to the cumulative reduction of the FEV. In addition, it states the cost of each measure per percentage of FEV-coverage, thus allowing a comparison. It stimulates scenario exploration and has been used in various ways: as consistency check of flood-mitigation plans by (local) governments, as a-priori and fast exploration of Nature Based Solutions (NBS) to flooding, and as an a-posteriori executive summary of complicated engineering design calculations of proposed flood defences. Two examples are explored further with an eye on incorporating and communicating more inherent uncertainty: one involving NBS for the River Glinščica near the city of Ljubljana in Slovenia and one involving NBS with spatial-temporal variations in rainfall and geographical locations for the NBS based on data of the River Don flood of 2007 in the city of Sheffield, UK. Limitations of the tool are analysed and suggestions for advancing the tool further are made.

3.1 Introduction and history

Both the 2015 Boxing Day floods in Leeds and the experience gained by designing and showcasing the Wetropolis flood demonstrator triggered the development of a novel science-policy tool on assessing the cost-effectiveness of flood-mitigation plans under development or already proposed, e.g., by government bodies. Possibly and hopefully such plans emerge in engaging, trustworthy and insightful discussions with the affected and interested public. A particular realisation was that several measures concern the effective or dynamic storage of floodwater volume. Hence, both exceedances of a threshold water level h_T as well as a threshold flood-excess dis-

charge Q_T need to be considered in tandem with the integrated difference $Q(t) - Q_T$ of discharge minus threshold discharge thus defining the FEV. Subsequently, FEV became a centre-piece of the tool since it can be related directly to cost-effectiveness, including individual and total costs of various measures proposed as well as their effectiveness expressed as respective flood volumes captured. Communication with the various stakeholders (i.e., including the public as stakeholder) involved in the decision-making process on flood mitigation measures is often a challenge because complicated engineering hydraulics and designs need to be summarised and translated in an understandable manner. The newly developed tool [3, 4] has proven to allow clear communication and engagement with stakeholders on various levels of sophistication, including usage as fast a-priori exploration, as sanity check of flood-mitigation plans and as a-posteriori communication in the form of an executive summary of intricate engineering design calculations.

A graphical overview of the tool is found in the schematic of Fig. 3.1. The starting point is the three-panel graph of Fig. 3.1a) in which basic water-level measurements are displayed in the third, bottom-left quadrant with time t going downwards and water level $h(t)$ on the axis going left, an axis shared with the rating curve displayed in the second, top-left quadrant with discharge $Q = Q(t)$ on the upward vertical axis, the latter vertical axis is in turn shared with the hydrograph displayed in the first, top-right quadrant with therein again time but now on a rightward-going, horizontal axis. Threshold level h_T displayed as a vertical line appears in both the third and second quadrants, linked in the latter second quadrant via the rating curve to threshold discharge Q_T as horizontal dashed line continuing also in the first quadrant. The fourth, bottom-right quadrant can serve as display for the various values and errors involved. In the hydrograph (first quadrant), the flood-excess volume (FEV) is the coloured or hatched area between threshold level Q_T and the time-dependent discharge $Q(t) > Q_T$. This FEV V_e can be displayed as a square lake, shown in Fig. 3.1b), with a human-size depth of $D = 2\text{m}$ and side lengths $L = \sqrt{V_e/D}$ such that the FEV equals the lake depth times the lake area, i.e. $V_e = DL^2$. To avoid flood damage, the cumulative effects of various flood-mitigation measures should preferably reduce the entire FEV to zero, assuming independence of each measure or anticipating overlapping effects. That square lake is thus partitioned in blocks, each representing the fraction of FEV covered by a particular mitigation measure; exemplified and displayed here are higher walls (HW in blue), giving-room-to-the-river (GRR in yellow) and floodplain storage (FPS in green). Since the square-lake depth $D = 2\text{m}$ tends to be shallow relative to the typical lake side length L on the order of a kilometre or so, the lake is best viewed from above as a square “pie” chart, with the measures appearing as rectangular blocks (or quadrilateral or triangular shapes). Added therein Fig. 3.1c) via double-sided arrows are the percentage covered of the total FEV (stated above the arrow) as well as the costs of each measure and the cost per percentage of that measure (given near the relevant arrow). In addition, total costs and total cost per percent can be displayed around a double-headed arrow across the lake-width. This graphical tool facilitates stakeholder participation in decision-making on flood protection, which participation is often hampered by a lack of enlightened communication on the technical complexities involved. Such [normative] “debates

are [often] not held in an open and inclusive way, incorporating the views of all stakeholders” [25]. The tool has hitherto proven to stimulate in-depth debates on flood-mitigation plans and exploration of various mitigation scenarios in the EU [39, 21], and was deemed valuable by involved EU stakeholders [9].

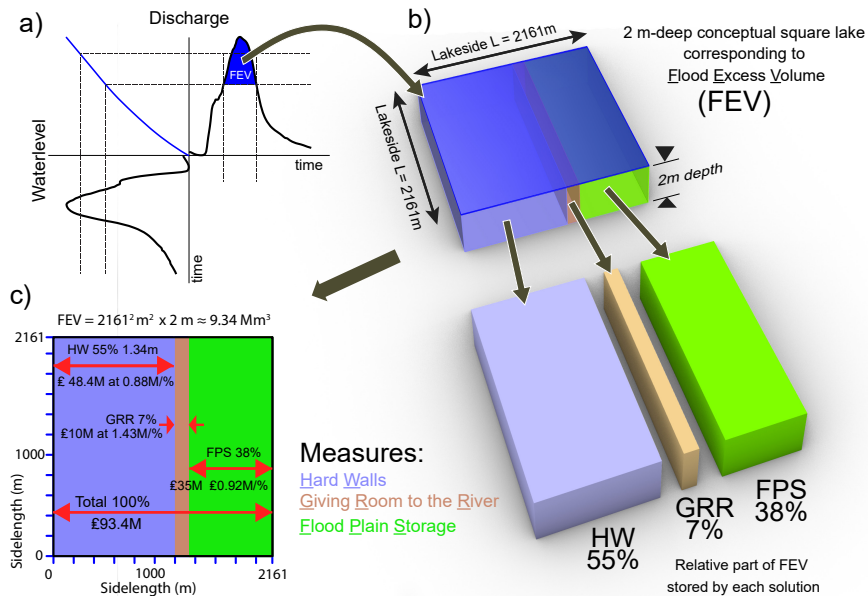


Fig. 3.1 A graphical overview of the square-lake cost-effectiveness tool based on flood-excess volume (FEV) consists of the following: a) a newly-compilated three-panel graph with the basic water-level measurements and rating curve results in a hydrograph with FEV (here similar in shape to the 2015 Boxing Day flood in Leeds at $9.34 \text{ Mm}^3/\text{s}$) indicated via shading; b) this FEV is expressed as a two-metre deep square lake and then partitioned into segments representing the coverage by each flood-mitigation measure; c) since the lake is so shallow relative to its typical side length (here $L = 2161\text{m}$), a square-lake “pie”-chart with costings and information of each measure, is established, facilitating further exploration in various cost-effectiveness scenarios with similar square-lake graphs which can be compared and interactively adapted in a flood-mitigation decision-making process. Courtesy sketch: Wout Zweers.

The tool was originally developed to both understand and serve as a sanity check of Leeds City Council’s flood-mitigation plans, which were proposed and developed in 2017-2021 after the 2015 Boxing Day floods of the River Aire [4, 8]. In addition, the tool was later used as a mixed a-priori and a-posteriori communication tool [3, 39] between engineers and stakeholders of a municipality in South-East France involved in flood-mitigation plans after devastating floods of the River Brague in 2015. The sanity check of these River Aire plans revealed some inconsistencies, which may have been surprising given the available limited information, but emerged by combining an analysis of the factual 2015 flood hydrograph with the proposed publicly available

mitigation plans. These inconsistencies were factually directly, repeatedly and duly reported to local and national UK flood government professionals before further and public dissemination in reports and peer-reviewed articles was undertaken [4, 21], the latter to be able to promote the tool outside Yorkshire. In the EU, the tool became part of the EU NAIAD network “*NAture Insurance value: Assessment and Demonstration*” in an assessment of NBS to flood mitigation, both in a more advanced analysis of the mentioned plans for the River Brague in France as well as in a fast a-priori analysis for the River Glinščica near the city of Ljubljana in Slovenia, see Parts 6 and 7 in [39]. A summary of the tool’s employment in these three realistic cases in the UK, France and Slovenia is provided in [9], accompanied by an in-depth discussion of its advantages and limitations.

In this chapter, to explain and exemplify the tool further, two cases will be revisited and extended:

- NBS to flood mitigation and ecological enhancement for River Glinščica floods will be assessed; both errors and (partly hypothesised) co-benefits will be added to the cost-effectiveness analysis in a graphical manner; and,
- two hypothetical yet realisable NBS flood-mitigation measures will be assessed for (constrained) spatial-temporally distributed rainfall and measures in the Upper Don valley based on data from the River Don flood of 2007, Sheffield, UK. This will extend (preliminary) work in the previous reports [39, 1]¹.

After analysing these two cases, a discussion will be given of the advantages and limitations of the tool, intertwined with the definition of a new protocol for assessing and communicating flood-mitigation plans in unison.

3.2 Visualisation of river data revisited

3.2.1 River Glinščica, Slovenia

The Glinščica is a small river in central Slovenia bordering the Ljubljana municipality to the East. Its catchment measures circa 17km² with about 23.200 inhabitants. The river has steep hill slopes in the upper catchment and floods occur in the flat agricultural and urban areas further downstream after high-intensity rainfall. Flooding and flood-mitigation options based on NBS have been studied as part of the EU project NAIAD [39, 36]. A (discharge) gauge along the river was dismantled in the 1990s so there are no river records over the last few decades. An extensive hydrological and hydraulic modelling effort was thus undertaken in which the water supply to these models was established after extensive rainfall analysis [39], including modelled peak discharges with 10, 100 and 500 year return periods or *AEP*’s of

¹ Both cases qualify as a-priori analysis. The analyses performed here have been redone and undertaken with a *Python* code made available on the GitHub site <https://github.com/Flood-Excess-Volume/RiverDon>; other branches therein contain *R*, *Matlab*, *Excel* codes for a variety of river floods and matching data.

(10, 1, 0.2)%. In contrast to the hydrographs based on measured data shown so far, only simulation data of discharge will be used and have been supplied together with a rating curve based on some tabulated values of water level and discharge at a critical downstream location. Water levels here are therefore reconstructed from the discharge with the rating-curve information via linear interpolation between two tabulated values². While water level is seen to be a monotonic function $h = h(Q)$ of discharge Q , the discharge may locally be a multivalued function of Q , cf. the top-left panel in the three-panel graph of Fig. 3.2. With the chosen and established thresholds of $h_T = 2.39\text{m}$, $Q_T = 29.5\text{m}^3/\text{s}$, the FEV becomes $V_e \approx 0.26\text{m}^3$. Based on a water-level error of 15%, estimates by the modelling experts, the FEV lies between $V_e = [0.22, 0.29]\text{m}^3$, indicated by the grey shading in the hydrograph –as seen in the top-right panel of Fig. 3.2. The flood duration T_f is circa 4.25hrs.

3.2.2 River Don flood 2007, UK

Excessive flooding of the River Don occurred on 25/26-06-2007 in Sheffield, South Yorkshire, UK, resulting in major damage and casualties [3]. To estimate and calculate the corresponding FEV, data from the gauge station Sheffield Hadfields are considered next. Gaugemap³ indicates that flooding is possible above 2.63m. In contrast to the River Armley and River Calder cases, less in-situ information is known to the author. Given that the EA's threshold level is quite low, as in the River Aire case for the Boxing Day 2015 floods (see [1]), the threshold level is increased to $h_T = 2.9\text{m}$ heuristically to obtain an initial estimate of the FEV. The corresponding time duration is $T_f = 13.5\text{hrs}$ with a concomitant $Q_{max} = 259\text{m}^3/\text{s}$, as follows from the data provided by the EA.

j	h_j m	c_j $\text{m}^3 \cdot \text{b}_j / \text{s}$	a_j m	b_j -
1	0.52	78.4407	0.223	1.7742
2	0.931	77.2829	0.3077	1.3803
3	1.436	79.5656	0.34	1.2967
4	3.58	41.3367	-0.5767	1.1066

Table 3.1 The coefficients c_j , a_j , b_j as well as the limb thresholds $h_0 = 0$ and h_j for $j = 1, 2, 3, 4$ for the rating curve at the river-level gauge station for the River Don at Sheffield Hadfields [15].

Detailed analysis of the River Don flood of 2007 using 15min–interval measurements is shown in Figs. 3.3 and 3.4 with the coefficients given in Table 3.1. The calculated excess volume for the threshold of $h_T = 2.9\text{m}$ yields

$$V_e(h_T = 2.9\text{m}) \approx (3.00 \pm 0.24)\text{Mm}^3 \quad (3.1)$$

² Water level simulation data matching the discharge data were no longer available.

³ Sheffield Hadfields available at: <http://www.gaugemap.co.uk/#!Detail/1854>

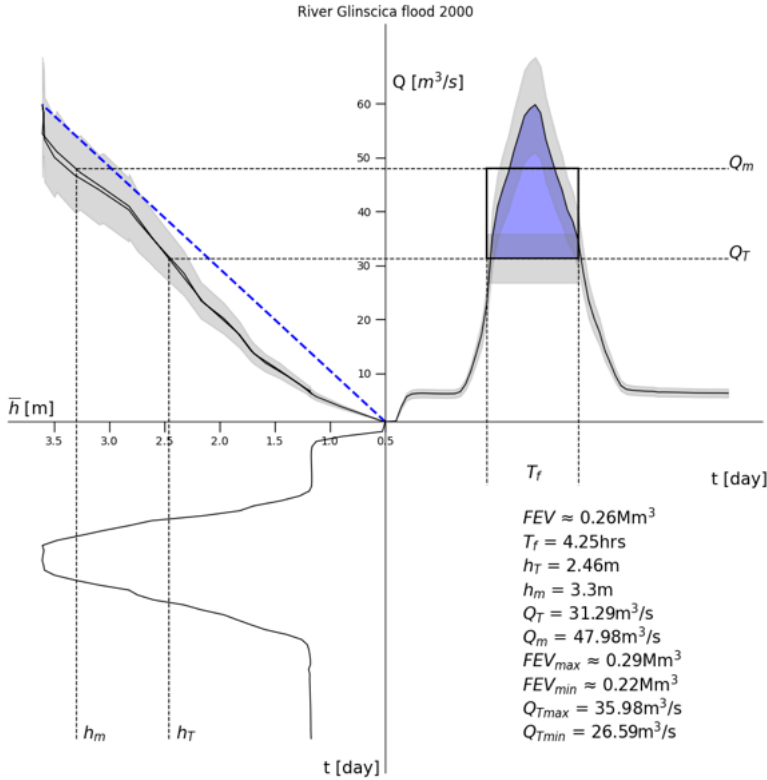
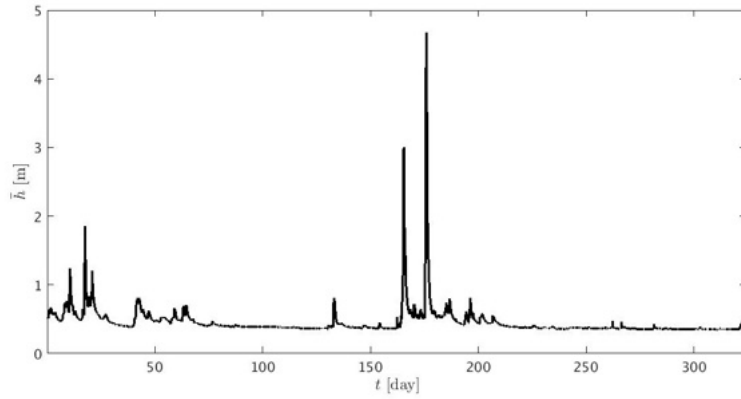


Fig. 3.2 A three-panel graph (cf. Fig. 3.1) displays the water levels as function of time, a rating curve, and discharge as function of time with the error bars based on a 15% error in the rating curve. Data are based on, e.g., simulated floods of the River Glinščica. Graph redone in *Python* based on data from G. Piton and A. Pagano. To do –optional: display tabulated curve as well and see if there is a minor glitch in the interpolation procedure. Start at origin?

or the capacity of a 2m-deep square lake of side-length 1225m or 0.74mi. By comparison with the sloping dashed line in the second quadrant in Fig. 3.3b), the rating curve therein is seen to be pseudo-linear for moderate to high depths. A quick estimate (2.9) of the FEV using a linear rating curve, giving $V_{e2} \approx 2.434Mm^3$, is roughly $2.434/3.00 \approx 81\%$ accurate. In contrast, the rating curves for the gauge stations at Armley and Mytholmroyd are more nonlinear (for respectively the Yorkshire rivers Aire and Calder, see [4, 3]), which explains the larger discrepancies with estimate

a)



b)

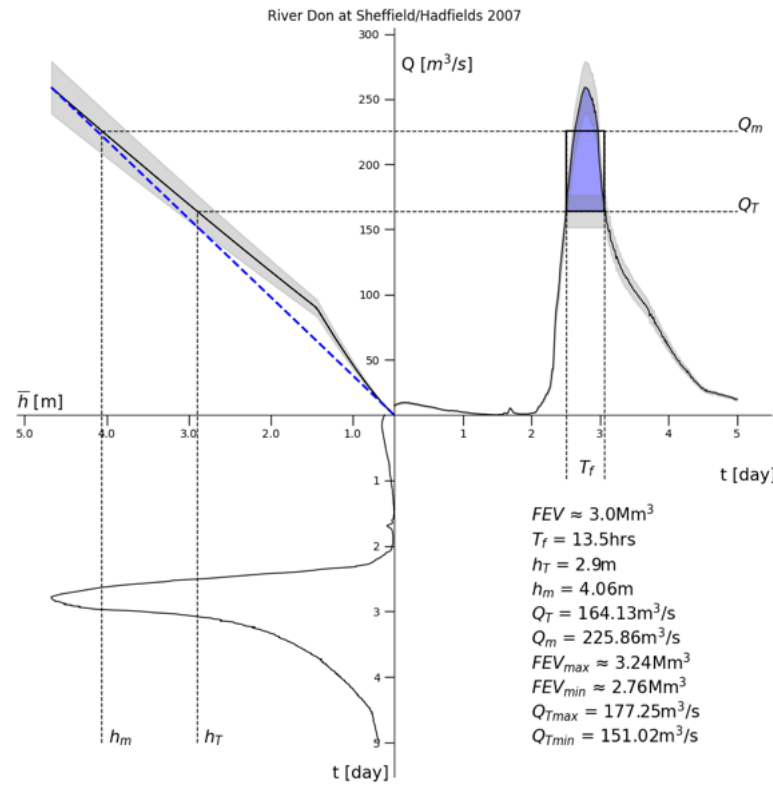


Fig. 3.3 Flow rate and river-level data of the River Don at Sheffield Hadfields: a) annual context (time unit: day from 01-01-2007) and b) exploded integrated visualisations (*cf.* Figure 3.1) around the 25-06-2007 floods (time unit: day).

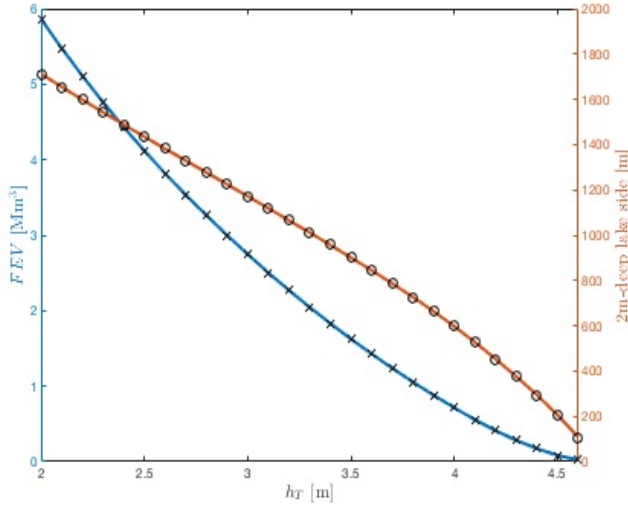


Fig. 3.4 River Don FEVs (left axis, crosses) and equivalent-square-lake sizes (right axis, circles) for various threshold levels h_T shows the dependence $V_e(h_T)$ of FEV on the chosen threshold level h_T . Data of the River Don at Sheffield Hadfields for the 25-06-2007 flood.

V_{e_2} , approximately 65% and 50% for those rivers, between the estimated and calculated flood-excess volumes for the chosen indicative river-level thresholds. Despite exhibiting quasi-linearity above $h_3 = 1.436\text{m}$, large error bars (circa 8%) at low depths (and even up to 20% below $h_2 = 0.931\text{m}$), are reported to be a common issue at the Sheffield Hadfields gauge [15], while no standard error has been calculated for the highest stage (h_4). In the above we have used the 8% error as a placeholder for the highest stage and beyond. The errors for the River Aire case are at most circa 5.5%, as noted in [4], and 13.6% for the River Calder. The variation of FEV and its associated square-lake size as function of h_T are displayed in Fig. 3.4. Varying h_T is seen to lead to roughly similar size errors as the error variation of FEV induced by errors in the rating curve.

3.3 A portfolio of Nature Based Solutions –NBS

3.3.1 River Glinščica

The goal in the demonstration for the River Glinščica within the NAIAD project has been to integrate both physical and stakeholder-driven models⁴. A wide group of stakeholders was identified and involved including, e.g., actors from the Slovenian Ministry for Environmental and Spatial Planning, other governmental institutions, recreational associations, city quarters, and civil initiatives. To reach that goal water-related flood risks have been assessed collectively in combination with an evaluation of the effectiveness of Nature Based Solutions (NBS) and their multiple benefits. NBS include river re-meandering, opening natural floodplains, using large dry retention areas, removing bridges, creating small multi-function wet retention areas, installing green roof rain-water tanks and removing crosswise barriers in the river bed. These lead to multiple benefits for society in this case study. Besides flood mitigation, dry and wet retention areas have recreational value near the City of Ljubljana for minor extra costs –costs used for creating and maintaining footpaths, information signs and such. Similarly, green roofs with their water tanks holding rainwater and thus reducing flood volume, can also be used to store water in longer drought periods and green roofs offer insulation against heat waves and cold spells. The use of these water tanks in droughts needs to be controlled to avoid the water tanks being used before major rain fall but use in longer dry spells is warranted.

The FEV-tool has been used in the Glinščica demonstration because it offered a fast a-priori investigation based on simulated hydrographs and cost-effectiveness visualisation comprehensible for the stakeholders involved. In addition, the anticipated combined hydrological groundwater modelling and hydraulic river channel modelling had not materialised in time such that the faster hydrograph-based FEV approach emerged as a viable alternative, even though it is less accurate. The next step is to consider the NBS involved and consider the cost-effectiveness of these measures in a square-lake graph.

3.3.2 River Don

Sheffield City Council (Sheffield CC, UK) aims to increase the flood protection against events such as the 2007 flood, which had a 1 : 200-year return period. This protection consists of a hybrid set of flood-mitigation measures, most of which have been completed. To offer further protection against enhanced flooding due to climate change, Sheffield CC is exploring NFM and NBS, e.g., in the form of 1521 attenuation features such as leaky dams as well as floodwater storage by drawing down the water levels of drinkwater reservoirs in the upper parts of the River Don catchment. It is

⁴ Various pieces of information in this section stem from [36] and a NAIAD-presentation shared with me by Polonal Pengal and Alessandro Pagano.

currently not clear what extra flood protection is required to mitigate against climate-change effects. Several studies, including [19], indicate that, for flood events with a return period larger than 1 : 100 years, there is no statistical evidence for increased flood intensity and volume due to climate change, while there is evidence that it increases for floods with return periods of less than 1 : 100 years. These findings may seem to contrast with the climate predictions in [43]; however, the latter predictions contain considerable uncertainties for the largest return period considered, *i.e.*, the 1 : 100-year one. That is, since flood protection against the 1 : 200-year return period flood is already in place, no further flood mitigation against climate uptake may be required as a consequence of this information. However, the 2021 IPCC report on climate change does predict more extreme rainfall events. Based on the FEV of the 2007 flood event, we analyse the extra flood-mitigation capacity offered by these proposed NFM and NBS but now regarding an idealised yet representative set of rainfall scenarios. It leads to the following more complex, yet more realistic, analysis.

3.3.2.1 NFM via circa 1500 leaky dams

Sheffield CC has performed a study of flood mitigation via NFM by using over 1500 flow-attenuation features [45]. It reveals that the available flood-storage volume V_d accumulated in 1521 flow-attenuation features such as leaky dams is $V_d = 0.567\text{Mm}^3$. Available flood-storage volume is denoted as “*volume of ‘new’ NFM storage*” in the report from [45]; therein ““*new*” is presumably relative to a basic storage volume for a 1 : 200-year return-period flood, even though that is not explicitly stated. Hence, assuming that this entire volume can be attained during such high-risk and high-volume flood events, including floods such as the 2007 one, it captures $V_d/V_e(h_T = 2.9\text{m}) = 0.567/3.00 \approx 18.9\%$ of the FEV (3.1). For higher-threshold values of h_T , this fraction is seen to be much higher, *cf.* Fig. 3.4. These estimates are of course upper bounds because the full volume of $V_d = 0.567\text{Mm}^3$ may not be attainable, either because part of this volume is already filled prior to the flood or because the rainfall is not uniform across the area covered by the flow-attenuation features. In addition, maintenance of the leaky dams and cascade failure need to be addressed, as in [18]. Despite these caveats, this upscaling of NFM features to 1521 dams shows that the cumulative effects to flood mitigation could be substantial. It warrants a pilot field study with hundreds of leaky dams, in order to monitor not only both their efficiency and durability but also the validity of accompanying modelling approaches.

3.3.2.2 Flood storage in reservoirs

Since 2017, the EA and Sheffield CC have been exploring the potential floodwater storage by drawing down various reservoirs, yielding an estimated storage volume of $V_r = 2.8\text{Mm}^3$. Summarised simply, contributions to flows in the Lower Don Valley (from downstream of the River Sheaf) are split approximately one-third each: via

the catchment area with the reservoirs; from the River Sheaf area, an area without any reservoirs; and, from the rest of the Upper Don catchment without the reservoir catchment⁵. The map in Fig. 3.5 of Sheffield City shows the catchment area in the East with the reservoirs and the River Sheaf area in the South. The Sheffield Hadfields gauge concerns the Lower Don Valley: hence, under more or less uniform rainfall and equal run-off times, this means that the part of the catchment with reservoirs concerns only $\frac{1}{3}$ of the FEV of $V_e(h_T = 2.9\text{m}) = 3.00\text{Mm}^3$ given in (3.1), i.e., $V_e/3 = 1.00\text{Mm}^3$ such that only part of the potential storage V_e can then be reduced. Reservoir storage under uniform rainfall is therefore in principle larger than the $V_d = 0.567\text{Mm}^3$ offered by the 1521 leaky dams. Whether it is possible to harness this flood-storage volume V_r in advance of an extreme-rainfall event depends on a series of factors, including the spatial rainfall distribution and the ability to draw down the reservoirs safely far enough in advance of rainfall predictions, while also balancing the need to keep these reservoirs sufficiently filled to maintain the drinking water supply. This requires further detailed modelling and pilot studies, involving active control of the hydraulics, cf. [10] and [47].

3.4 Cost-effectiveness analysis viewed as square-lake graphs

3.4.1 River Glinščica

In the River Glinščica investigation of flood-mitigation measures, four types of NBS have been considered to accommodate the relevant FEV (reduction) of circa 0.278Mm^3 (i.e., this value lies within the FEV-range, cf. Fig. 3.2), as follows:

- urban wet retention areas with an available flood-storage volume of $V_1 = 24984\text{m}^3$, i.e. 9%, at a cost of $300\text{k}\epsilon$;
- green roofs with an available flood-storage volume of $V_2 = 26200\text{m}^3$, i.e. 10%, at a cost of $5.24\text{M}\epsilon$;
- opening flood plains with an available flood-storage volume of $V_3 = 42780\text{m}^3$, i.e. 16%, at a cost of $548\text{k}\epsilon$; and,
- dry retention areas with an available flood-storage volume of $V_4 = 184194\text{m}^3$, i.e. 66%, at a cost of $2.0\text{M}\epsilon$.

The corresponding square-lake cost-effectiveness graph is found in Fig. 3.6, first by ignoring any co-benefits and purely considering flood-mitigation benefits. Hence, all costs have been attributed towards the budget for flood mitigation despite multiple co-benefits warranting a distribution of costs over several cost items. Note that the cost per percentage of green roofs is at 524k nearly 18 times higher than the costs per percentage of circa 32k for the other measures. Consequently, a large part of the total costs of circa 8.1M stems from the green roofs.

⁵ The simplification presented is based on correspondence with Simon Byrne and James Mead from the Yorkshire EA; our analysis merely serves to illustrate the use of FEV.

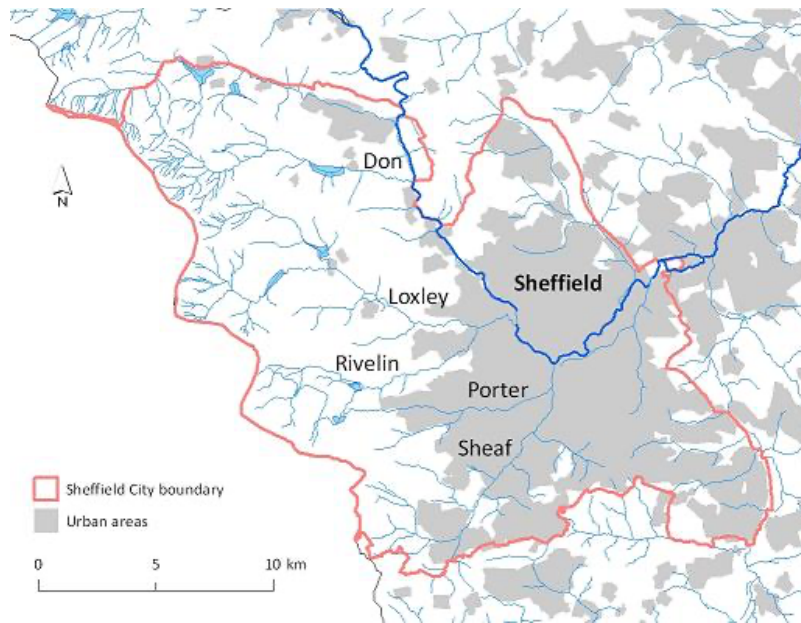


Fig. 3.5 The Sheffield City catchment area with the reservoir area in the East, with multiple reservoirs, the River Sheaf area in the South and the main urban area of Sheffield. The River Don is indicated with a dark blue line and smaller tributaries with thin light blue lines. The Sheffield City boundary is indicated in red. <https://www.sheffield.ac.uk/doncatchment/about> © Crown Copyright/database right 2011; an Ordnance Survey/EDINA supplied service; river layer kindly licensed from the EA. Courtesy: To do or sufficiently acknowledged?

It is therefore of particular interest to consider the potential of multiple benefits for green roofs and explore how such co-benefits can be displayed graphically. Lacking actual figures, the multiple benefits of green roofs are hypothetically distributed: a) half over flood mitigation by storing water in water tanks, emptied prior to (extreme) rainfall, b) one-third over storage in water tanks for use in drought periods and c) one-sixth over the insulation value of green roofs against heat and cold spells, thus saving on heating and/or air-conditioning costs. Costs are likewise distributed over three cost items, thus cutting the flood-mitigation costs per percentage of FEV covered by one-third. This is the honest, factual way of disseminating the budget over three items, while in practice flood-mitigation has been topical since there is government money available. The consequence is that co-benefits of a flood-mitigation measure are often slotted entirely under the budget for flooding in order to fund these other benefits. Such a strategy is not transparent and has led to argumentations in favour of certain flood-mitigation measures which are not warranted by the effectiveness of the measure for flood mitigation.

The heavy promotion of beaver colonies in the UK (by certain media, and in certain government and academic circles) as an important measure to prevent floods

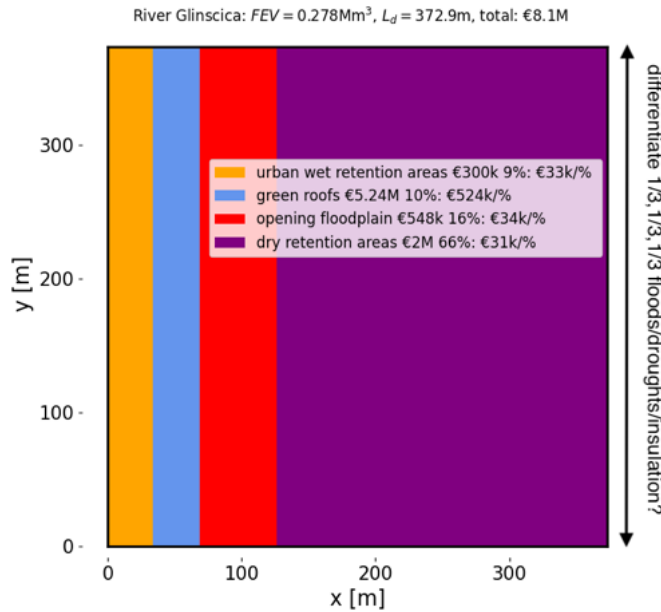


Fig. 3.6 Displayed is the square-lake cost-effectiveness graph for NBS to the River Glinščica, involving urban wet retention areas, green roofs, opening flood plains and dry retention areas. All costs involved have been put only on a flood-mitigation budget as in [36]. Graph redone in *Python* based on data from G. Piton and A. Pagano.

in order to guarantee its funding via the flooding budget has been discussed in Chapter 2. The flood-prevention value of beaver colonies was shown to be minute and upscaling remains unrealistic. The flood benefits of beaver colonies have presumably been exaggerated in order to ensure funding for the actual main benefit of wildlife enhancement⁶. Such promotion has also led to misconceptions with the general public about the flood-mitigation potentials of beaver colonies. Factual dissemination of the costs over the multiple benefits and clear communication thereof would dispel such misconceptions.

While flood benefits are the main benefits of NBS in the Glinščica, that was not the case in a study at three sites along the River Danube [38]. Therein it turned out that the main economic benefit was the recreational value of the NBS studied, a value initially rendered as a co-benefit. The relative benefits of various flood-mitigation measures in [38] have been displayed clearly via histograms of the costs per co-benefit for each site. In Fig. 3.7 such co-benefits are included graphically for the

⁶ Promotion of the beaver colony in the Finchingfield Brooke catchment was indeed admitted to be a pr-strategy –private communication at the 2019 Flood and Coast conference.

green roofs considered in the Glinščica case study. The total costs attributed to flood benefit are seen to lower from 8.1M to 5.45M.

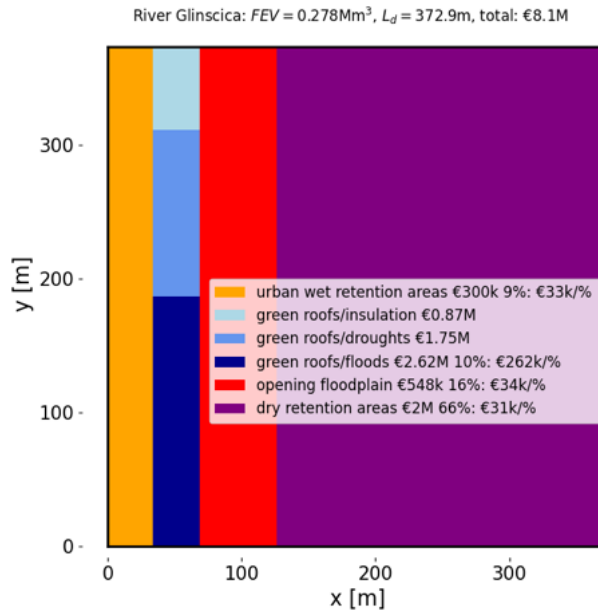


Fig. 3.7 Displayed is the square-lake cost-effectiveness graph extended to include the relative contributions of co-benefits for green roofs for the River Glinščica, involving four NBS: urban wet retention areas, green roofs, opening flood plains and dry retention areas. The different shadings of blue display the co-benefits and costs of green roofs, in which the lighter shades of blue indicate a lower cost fraction.

Citing [36], who conclude very clearly and aptly as follows: “*Stakeholders eventually agreed that the developed strategy for water risk mitigation using NBSs in the Glinščica catchment is a viable alternative to existing grey infrastructure plans. However, the participatory process revealed several barriers to mainstreaming NBS and implementing an adaptive management approach in Slovenia, mostly in the governing and institutional systems. Through the participatory planning process, we built capacity and changed the perceptions of participating stakeholders regarding NBSs and their efficiency in providing multiple co-benefits in addition to the flood protection, which is usually the only function and benefit of grey measures*”.

3.4.2 River Don

To illustrate a more complex flood-mitigation analysis, we hypothesise several idealised precipitation scenarios, divided seasonally over the autumn and winter (hereafter abbreviated as “winter”) as well as spring and summer (hereafter abbreviated as “summer”) seasons, and over the three catchment areas. Each precipitation scenario is assumed to lead to a resulting FEV of $V_e = 3.00\text{Mm}^3$ further downstream of the River Don at Sheffield Hadfields and we will state how the fractions of the FEV are distributed across these three roughly equal-sized areas. The three catchment areas introduced above will be denoted by a “reservoir” area with a cumulative flood-storage volume of $V_r = 2.8\text{Mm}^3$, a “Sheaf” area with no additional flood-storage volume and an “upper Don” area with available flood-storage volume stored behind leaky dams with a cumulative available flood-storage volume of $V_d = 0.567\text{Mm}^3$. For a map of the catchment, see Fig. 3.5.

In order to describe and quantify the scenarios, a “rainfall fraction” vector (RFV) and corresponding notation $(\alpha, \beta, 1 - \alpha - \beta)$ is introduced, with $0 \leq \alpha, \beta \leq 1$ and $0 \leq \alpha + \beta \leq 1$, to indicate weights of the relative rainfall in the above-defined (reservoir, Sheaf, upper Don) areas. For example, the rainfall vector $(\frac{1}{3}, \frac{1}{3}, \frac{1}{3})$ signifies that rain has fallen uniformly across all three areas, each catching a third of the FEV, while $(\frac{1}{2}, \frac{1}{2}, 0)$ means that rainfall was evenly distributed across only the reservoir and Sheaf areas but not the upper Don area; similarly, $(0, 0, 1)$ means that all rain fell in only the upper Don area.

The various rainfall scenarios considered below (and summarised in Table 3.2) are somewhat arbitrary but are chosen such that, in winter, more coherent larger-scale rainfall patterns are favoured relative to the summer, which is itself prone to having more isolated rainfall patterns. Seven different spatially distributed scenarios for an extreme flood with FEV $V_e = 3.00\text{Mm}^3$ are now readily described by their respective RFVs and listed below; for later use, they are also assigned corresponding seasonal probabilities of occurrence, as follows:

- S1: spatially uniform ‘large-scale’ rainfall with the single RFV option $(\frac{1}{3}, \frac{1}{3}, \frac{1}{3})$, which is assigned a probability of 50% in the winter and 25% in the summer; in an obvious notation, $p_{S1,w} = \frac{1}{2}$ and $p_{S1,s} = \frac{1}{4}$.
- S2: rainfall localised to only two of the three sites with RFV options (a) $(\frac{1}{2}, \frac{1}{2}, 0)$, (b) $(0, \frac{1}{2}, \frac{1}{2})$ or (c) $(\frac{1}{2}, 0, \frac{1}{2})$. For winter, the first two combined are given a 25% probability of occurrence, such that $p_{S2(a),w} = p_{S2(b),w} = \frac{1}{8}$, and (c) is assigned zero probability, $p_{S2(c),w} = 0$. For summer, the three options combined have a 25% probability of occurrence, such that $p_{S2(a),s} = p_{S2(b),s} = p_{S2(c),s} = \frac{1}{12}$.
- S3: extreme rainfall localised to just one location with RFV options (a) $(1, 0, 0)$, (b) $(0, 1, 0)$ or (c) $(0, 0, 1)$, given a combined 25% probability in the winter and a combined 50% probability in the summer, such that $p_{S3(a),w} = p_{S3(b),w} = p_{S3(c),w} = \frac{1}{12}$ and $p_{S3(a),s} = p_{S3(b),s} = p_{S3(c),s} = \frac{1}{6}$.

To facilitate the presentation and quantification of the analysis, the above RFVs and volumes per scenario and area may be readily summarised in the following matrix

representations (truncated to a maximum of three decimal places), with row-wise scenarios and column-wise locations:

$$A_{rf} = \begin{pmatrix} \frac{1}{3} & \frac{1}{3} & \frac{1}{3} \\ \frac{1}{2} & \frac{1}{2} & 0 \\ 0 & \frac{1}{2} & \frac{1}{2} \\ \frac{1}{2} & 0 & \frac{1}{2} \\ 1 & 0 & 0 \\ 0 & 1 & 0 \\ 0 & 0 & 1 \end{pmatrix} \quad \text{and} \quad A_r = V_e A_{rf} = \begin{pmatrix} 1 & 1 & 1 \\ 1.5 & 1.5 & 0 \\ 0 & 1.5 & 1.5 \\ 1.5 & 0 & 1.5 \\ 3 & 0 & 0 \\ 0 & 3 & 0 \\ 0 & 0 & 3 \end{pmatrix} \text{Mm}^3. \quad (3.2)$$

The corresponding storage matrix reads

$$A_s = \begin{pmatrix} V_r & 0 & V_d \\ V_r & 0 & V_d \end{pmatrix} = \begin{pmatrix} 2.8 & 0 & 0.567 \\ 2.8 & 0 & 0.567 \\ 2.8 & 0 & 0.567 \\ 2.8 & 0 & 0.567 \\ 2.8 & 0 & 0.567 \\ 2.8 & 0 & 0.567 \\ 2.8 & 0 & 0.567 \end{pmatrix} \text{Mm}^3. \quad (3.3)$$

The amount of possible storage A_m in each area is the minimum of the storage matrix A_s and the volume matrix per scenario A_r . For the rainfall scenarios considered herein, it is given by

$$A_m = \min(A_s, A_r) = \begin{pmatrix} 1 & 0 & 0.567 \\ 1.5 & 0 & 0 \\ 0 & 0 & 0.567 \\ 1.5 & 0 & 0.567 \\ 2.8 & 0 & 0 \\ 0 & 0 & 0 \\ 0 & 0 & 0.567 \end{pmatrix} \text{Mm}^3. \quad (3.4)$$

The sum of each row of A_m yields the elements of total storage vector \mathbf{r}_v for each rainfall scenario, also given as a fraction of the FEV by the vector \mathbf{r}_{vf} , as follows

$$\mathbf{r}_v = (1.567, 1.5, 0.567, 2.067, 2.8, 0.0, 0.567)^T \text{ Mm}^3 \quad \text{and} \quad (3.5a)$$

$$\mathbf{r}_{rf} = \mathbf{r}_v / V_e = (0.5223, 0.5, 0.189, 0.689, 0.933, 0, 0.189)^T \quad (3.5b)$$

with transpose $(\cdot)^T$. Finally, the probability distributions assigned to the seven scenarios in winter and summer are summarised in the vectors

$$\mathbf{v}_w = (\frac{1}{2}, \frac{1}{8}, \frac{1}{8}, 0, \frac{1}{12}, \frac{1}{12}, \frac{1}{12})^T \quad \text{and} \quad (3.6a)$$

$$\mathbf{v}_s = (\frac{1}{4}, \frac{1}{12}, \frac{1}{12}, \frac{1}{12}, \frac{1}{6}, \frac{1}{6}, \frac{1}{6})^T, \quad (3.6b)$$

with components summing to unity.

Scenario	Rainfall fraction			Probability	
	Reservoir	Sheaf	Upper Don	Winter	Summer
S1	$\frac{1}{3}$	$\frac{1}{3}$	$\frac{1}{3}$	$\frac{1}{2}$	$\frac{1}{4}$
S2(a)	$\frac{1}{2}$	$\frac{1}{2}$	0	$\frac{1}{8}$	$\frac{1}{12}$
S2(b)	0	$\frac{1}{2}$	$\frac{1}{2}$	$\frac{1}{8}$	$\frac{1}{12}$
S2(c)	$\frac{1}{2}$	0	$\frac{1}{2}$	0	$\frac{1}{12}$
S3(a)	1	0	0	$\frac{1}{12}$	$\frac{1}{6}$
S3(b)	0	1	0	$\frac{1}{12}$	$\frac{1}{6}$
S3(c)	0	0	1	$\frac{1}{12}$	$\frac{1}{6}$

Table 3.2 Summary of the seven precipitation scenarios, with rainfall fraction for the three locations, and seasonal probabilities.

The average flood storage attained by the two flood-mitigation measures in winter and summer are given by the inner products $m_1 = \mathbf{r}_{rf} \cdot \mathbf{v}_w = 0.4408 = 44.08\%$ and $m_2 = \mathbf{r}_{rf} \cdot \mathbf{v}_s = 0.4325 = 43.25\%$ respectively. The spread between the extra flood mitigation offered for each rainfall scenario (N.B. by only the leaky dams and reservoir-mitigation measures considered here — Sheffield is protected by other measures) is quite extreme since, in both winter and summer, 0% flood protection occurs when rain falls in only the Sheaf area (*cf.* scenario S3(b)), with a chance of $\frac{1}{12}$ and $\frac{1}{6}$ in winter and summer, respectively, while 93.3% flood protection occurs when rain falls in only the reservoir area (*cf.* scenario S3(a)) with probabilities of $\frac{1}{12}$ and $\frac{1}{6}$ in winter and summer respectively. The standard deviations in the winter and summer are respectively $s_w = s_1 = 0.1751 = 17.51\%$ and $s_s = s_2 = 0.1638 = 16.38\%$, and are calculated as follows $s_i = \frac{1}{6} \sum_{j=1}^7 (m_i - v_{i,j})^2$ for $i = 1, 2$.

In Fig. 3.8, the above information is presented graphically for both winter and summer cases in terms of partitioned square ‘flood-excess lakes’ of the same volume as the FEV. These lakes are overlaid by not only the mean flood mitigation offered (and its standard deviation) but also the protection offered per rainfall scenario. This graphical interpretation of the analysis illustrates the fraction of FEV accounted for by each scenario in a concise and quantifiable manner and enables the reader (or stakeholder) to make informed choices when assessing potential flood-mitigation schemes.

For our hypothetical scenarios, we conclude that the proposed and current flood-mitigation measures, comprising NFM measures and the use of storage reservoirs, offer significant extra reduction (circa 45%) of flood levels based on the 2007 flood data, but their variance over the idealised rainfall distributions is, at circa 17%, relatively large. A significant portion of the volume is captured by the use of storage reservoirs (*cf.* scenarios 1, 2(a,c), 3(a)). Local knowledge of the catchment (from the EA) — that the lower River Don catchment is fed by water flow from three sub-catchments of roughly equal area, feeding into the Lower Don Valley where the Sheffield Hadfields’ river gauge is located — has been used to simplify and carry out the analysis. Even within those simplifications one could further refine the analysis

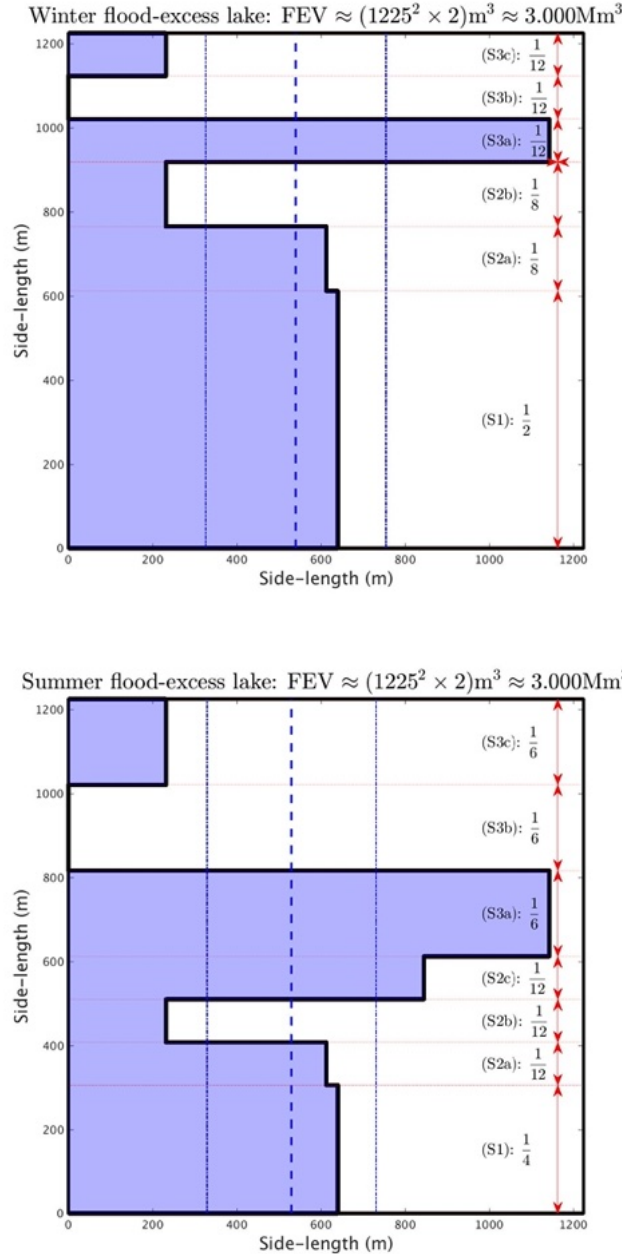


Fig. 3.8 A graphical overview of the fraction of the FEV captured by the two flood-storage measures, reservoirs and leaky dams in the reservoir and Upper Don areas of the Don catchment, respectively, for (top) the winter-rainfall scenarios and (bottom) the summer-rainfall scenarios. Stacked vertically are the respective probability distributions implied by the components of \mathbf{v}_w and \mathbf{v}_s in (3.6), relative to the associated FEV, which is fixed for all scenarios. The blue shaded areas to the left of the thick, stepped, solid line denote the fractions of the FEV mitigated per scenario, to be read horizontally (e.g., 93.3% for (S3a)). The mean FEV (winter 44.08%, summer 43.25%) over all seven scenarios and standard deviation (winter 17.51%, summer 16.38%) are indicated by thick and thin vertical dashed lines respectively.

by using realistic rainfall distributions, discretised using a piecewise-constant representation for the seven seasonally adjusted partitions. The seven scenarios could also be further refined. It should be noted that the starting point of the analysis is that each rainfall event leading to a 1:200-year return period flood event at Sheffield Hadfields had the same FEV as the 2007 flood. However, this does not necessarily imply that the total rainfall was the same in each scenario.

The framework offered by the FEV matrix representations and subsequent interpretation (*cf.* Fig. 3.8) is simple yet elegant: information covering a range of rainfall scenarios, mitigation measures, and geographical areas of a river catchment is encapsulated in a single graphic. Moreover, it is highly flexible and can incorporate any number of scenarios, rainfall distributions, and locations; indeed, the process used to produce Fig. 3.8 has been fully automated in anticipation of being utilised to examine other scenarios.

Finally, the probabilities used should really be obtained from a detailed analysis combining meteorological observations, weather, groundwater and river flow forecasts and simulations. Nonetheless, our idealised set-up in which rainfall is binned in a few subcatchments offered insight in the influence of spatio-temporal and even seasonal varying rainfall on the variation in efficacy of flood-mitigation measures. Due to the modelled uncertainty the square-lake graphics become more involved while the mean values still offer the original simplicity. Costs and costs per percentage covered can, of course, still be overlaid, as in the River Glinščica case study and published examples [3, 4, 9].

3.5 Limitations, extensions and inclusion of uncertainty

The graphics-based approach developed and displayed to communicate cost-effectiveness of flood-mitigation plans is on purpose relatively straightforward, in order to promote comprehension for and access to a large group of people. The cost-effectiveness tool can be used as consistency check of flood-mitigation plans, as fast a priori initial exploration of such plans or as an a posteriori executive summary of complicated engineering design calculations. As a consequence, it has been successfully used in the EU in French and Slovenian municipalities. However, that simplicity may also lead to some limitations, discussed next. By itself alone, the approach is not a flood-mitigation methodology but the approach forms part of the chain of steps for designing, choosing and implementing flood defences. Some of the limitations can be lifted by developing the approach further.

In most applications and examples of the tool investigated, water levels and a hydrograph of a single flood event at one location formed the basis to calculate the FEV and square-lake cost-effectiveness analysis. These data either originated from measurements or hydraulic simulations. While real flood data depend on space and time and are four dimensional, the FEV is zero-dimensional in space and only time dimensional. As explained in Chapter 1, when flood data are chosen at a suitable location then the approach obtains a one-dimensional reach along the stretch of river

over which the subcritical flow is controlled by the hydraulics of a nearby weir or rapid where the flow becomes critical as part of a sub/supercritical transition.

Another objection raised is that the FEV and cost-effectiveness approach is based on flood-storage volumes, both for the FEV and flood-mitigation measures, and as such ignores measures based on water-level heights and on slowing down the flow. Examples of such water-level measures are: higher flood-defence walls, levees, dikes and berms; and, examples of slowing-the-flow measure, favourably altering the hydrograph, are: leaky dams, giving-room-to-the river (e.g., riverbed widening and lowering as well as opening old river meanders), and passive and dynamic flood-plain storage due to weirs or constrictions possibly combined with moveable elements to exert control of constriction width or weir height. This objection is a misconception since FEV is a hydrograph-based concept therefore including changes in the FEV due to changes in the hydrograph induced by the implementation of flood-mitigation measures as in all slowing-the-flow examples. The calculated change of the hydrograph due to GRR is an explicit and analytical example showing how the threshold Q_T is raised to $Q_{T,GRR}$ due to GRR, thus reducing the FEV from the original V_e to $V_{e,GRR}$, see [3]. In effect, the original hydrograph and new hydrograph are subtracted with this straightforward threshold change. However in most of the simple a-priori applications shown, the explicit change of the hydrograph is not calculated but the FEV is simply partitioned in subvolumes associated with each flood-mitigation measure. Often, extensive calculations or data records for the situations prior to and after implementation of new flood-mitigation measures are not available, or not made available, for comparison. In such cases, a-priori use of the new tool with its inherent limitations is the only option, one still providing valuable insights. However, in the luxurious situation for which detailed calculations and/or simulations are available of the situation before and after the implementation of new flood-mitigation measures, then a-posteriori application of the cost-effectiveness tool leads to more rigour and can be extended in a major fashion. Given the coupling between the threshold discharge Q_T and the threshold water level h_T , the FEV-based approach does include the effect of water-level measures. Moreover, if simulations are available the strategy is to implement the measures related to FEV-reduction first and use any simulated excess water levels to determine the height of floodwalls, levees or berm heights. If simulations are not available, then this height follows roughly from the excess discharge above Q_T via the rating curve or height-flow data.

Flood-mitigation plans include various aspects of uncertainty. In the FEV cost-effectiveness analysis examples considered, the following uncertainty aspects have been included, together or in separation:

- When water-level data were combined with a rating curve based on a more intermittently measured combination of flow and water-level data, errors in the rating curve yielded an FEV with most often large error bars, typically between 10% and 50%, see Figs. 3.2, 3.4 and [3]. These errors were not carried further into the square-lake cost-effectiveness analysis.
- Co-benefits of a flood-mitigation measure can spread the costs over various budget items, as seen in Fig. 3.7 for the extended River Glinščica case study and in Perosa

- et al.⁷ [38]. The factual costs for the flooding budget does then get reduced even though overall costs remain the same.
- Spatially and temporally distributed flood-mitigation measures subject to spatial-temporal rainfall generally reduce the effectiveness of measures: when it does not rain or rains less upstream of a mitigation measure in the relevant river subcatchment, then the measure does not contribute, or contributes less, to reducing the relevant FEV further downstream. This was illustrated in the River Don example with its summer- and wintertime square-lake graphs shown in Fig. 3.8, in which uncertainty was captured by a combined effect of the spatial coverage of precipitation and the location of a flood-mitigation measure on the vertical axis of the square-lake graph. A major simplification, and as such a shortcoming, therein was the assumption that the precipitation timing was taken as the arrival of the rainfall volume at the downstream site in the city of Sheffield for which the FEV was calculated. Hence, details of the hydrological or groundwater and channel or hydraulic flow routes and travel times from the areas where precipitation falls to the bespoke location in Sheffield were ignored in this illustrative scoping analysis. Obviously, an a-posteriori analysis should be based on detailed flow calculations such as to obtain travel times and flow routes which would then determine the probabilities of rainfall volumes reaching Sheffield. In the case study these probabilities were estimated on an ad-hoc basis. Such a detailed study would be a major and worthwhile undertaking.
 - The use of single hydrographs, even when capturing the rating-curve errors, falls short of capturing more of the inherent uncertainty in the hydrograph associated with a particular chosen return period or AEP of an extreme flooding event. To capture this uncertainty, it is necessary to either have a data record with an ensemble of floods for a chosen event magnitude/AEP or to have an ensemble of detailed flood simulations for that AEP. That would lead to a spaghetti diagram of flood hydrographs with a mean and a standard deviation, leading to a mean FEV and FEV standard deviation. Such an ensemble approach does factually lead to a novel roadmap for a new FEV cost-effectiveness protocol for improved design and communication of flood-mitigation plans. That protocol has been described in detail in [4]. It aims to lead to better flood-mitigation designs and implementations.

Briefly, such a new roadmap consists of various steps. Step one is to choose protection in an area, e.g. a city, against a flood event with a chosen APE. Step two, using ensemble simulations, the associated FEVs and their uncertainty are calculated. After choosing and implementing one or a few flood-mitigation measures in the models, for example based on a fast a-priori cost-effectiveness analysis, detailed ensemble simulations are undertaken to calculate the new hydrographs for the same target AEP, resulting in possibly zero FEVs when these first flood-mitigation designs are seen to be appropriate. Preferably extra simulations are run to gauge the effects of a flood-mitigation measures considered in isolation, to see if combined flood-mitigation measures have diminished or increased effectiveness. When the FEVs are nonzero,

⁷ I had asked Perosa et al. to display the relative benefits more clearly.

new flood-mitigation scenarios are designed and tested again using ensemble simulations till results with sufficient convergence are reached, yielding FEVs close to or less than zero, or when computational time runs out. The relative simplicity of the graphical cost-effectiveness graphs can still be maintained to communicate with stakeholders, including the general public, by displaying the mean results of such advanced engineering design simulations. In addition, more advanced graphs including the acquired information on the uncertainty can be devised along the lines developed here and in [3, 4, 9]. The above novel roadmap shares similarities with data assimilation approaches in Numerical Weather Prediction and has, to the best of my knowledge, not been used in flood-mitigation planning.

Finally, it is important to emphasise that the tool discussed is a *cost-effectiveness* analysis and not a *cost-benefit* analysis. The effectiveness pertains to the FEV reduction by each individual flood-mitigation measure and the cumulative effectiveness of all measures combined. In a cost-benefit analysis (CBA), an economic assessment methodology is required to calculate the flood damages saved over a suitable period of time (say n_T years counted from the zero year of implementation), cost of implementation and maintenance, gains by multiple benefits of flood-mitigation measures and “*opportunity costs*” foregone because a flood-mitigation measure takes out production, e.g. via land use, see [13]. In the end, these aspects are expressed in monetary values. To obtain a quantifiable measure, [13] introduces a benefit-cost-ratio (BCR), as follows

$$BCR = \frac{\sum_{n=0}^{n_T} (AD_n + CB_n)/(1+r)^n}{\sum_{n=0}^{n_T} (C_n + OC_n)/(1+r)^n} \quad (3.7)$$

with CB_n the co-benefits in year n , AD_n the avoided damage in year n , r is a discounting factor expressing that individuals give a higher value to a present benefit than a future one as based on welfare economics – r is typically 3% to 5% [17], and C_n and OC_n are implementation and opportunity costs. A BCR larger than unity signifies economical efficiency of the project, leading to more economic welfare, and it should then be considered favourable to investments. An interesting question is whether it is possible and useful to develop graphical counterparts for such a CBA, using the BCR and other indicators such as defined in [13], accessible to a larger audience of stakeholders and akin to the ones used in the FEV-based cost-effectiveness analysis discussed in this chapter, in order to enhance and explore scenario thinking. In [13], the River Brague floods of 2015 were analysed in one of their cases studies such that the cost-effectiveness and cost-benefit analyses could be intercompared. While a cost-benefit analysis is better and preferred, the information required may not be available and is harder to obtain, and values such as AD_n , CB_n , C_n , OC_n and, hence, the BCR generally contain considerable uncertainties, such as reported in [13].

Chapter 4

Wetropolis flood demonstrator

Abstract Hallo

4.1 Tour of Wetropolis

- Description and statistics
 - Photos
 - goals
 - Dashboard

4.2 Modelling Wetropolis: designing versus predicting

Check and use with write-up to date.

4.2.1 Saint-Venant equations

- Spatio-temporal rainfall extremes: total in system, total per location, mixed model
 - Combined river, old or new groundwater model (?), reservoir and canal dynamics (new with Tom Kent).

4.2.2 Design model

4.3 Extreme Wetropolis' floods

4.3.1 Design model results

4.3.2 Predictive model results

(New)

4.4 Flood-excess volume and square-lake graphs

To do: new.

4.5 Outlook: data assimilation and flood control

- Simple model of dynamics and control

4.6 Redesign

Droughts and floods. More realistic river-level (relative) ranges.

Done in EGU2019 poster by me.

Appendix

4.6.1 Design model

4.6.2 Predictive model

Chapter 5

Discussion and outlook

Abstract Hallo; not sure if this chapter will be included or not.

References

1. Bokhove, O., Kelmanson, M., Kent, T.: On using flood-excess volume to assess natural flood management, exemplified for extreme 2007 and 2015 floods in Yorkshire. <https://eartharxiv.org/repository/view/1282/> (2018).
2. Bokhove, O., Kelmanson, M., Kent, T.: Using flood-excess volume in flood mitigation to show that upscaling beaver dams for protection against extreme floods proves unrealistic. Version July 2018: <https://eartharxiv.org/w9evx/> (2018).
3. Bokhove, O., Kelmanson, M., Kent, T., Piton, G., Tacnet, J.-M.: Communicating nature-based flood-mitigation schemes using flood-excess volume. *River Research and Applications* **35**, 1402–1414 (2019).
4. Bokhove, O., Kelmanson, M., Kent, T., Piton, G., Tacnet J.-M.: A cost-effectiveness protocol for flood-mitigation plans based on Leeds' Boxing Day 2015 floods. *Water* **1(2)**, 217–258 (2020).
5. Bokhove, O., Hicks, T., Zweers W., Kent, T.: Wetropolis extreme rainfall and flood demonstrator: from mathematical design to outreach and research. *Hydrology and Earth System Sciences* **24(5)**, 2483–2503 (2020).
6. Bokhove, O., Kelmanson, M., Kent, T.: A new tool for communicating cost-effectiveness of flood-mitigation schemes. UK Government inquiry on flooding. <https://committees.parliament.uk/writtenEvidence/9641/pdf/> (2020).
7. Bokhove, O., Kent, T., Piton, G.: Flood-excess-volume. Using “flood-excess volum” to assess and communicate flood-mitigation schemes: case studies including source code (Matlab, R, Excel and Python) and output. GitHub site: <https://github.com/Flood-Excess-Volume> (2020-2021).
8. Bokhove, O.: Wetropolis Design 2016-present and Wetropolis spin-off projects. GitHub site: <https://github.com/obokhove/wetropolis20162020> (2019-2021). An example of a spin-off includes a formal representation on flood-easing plans of Leeds City Council in my own village of Apperley Bridge¹.
9. Bokhove, O. 2021: On communicating cost-effectiveness of flood-mitigation schemes. ESREL Conference proceedings. 8 pp. <https://www.rpsonline.com.sg/proceedings/9789811820168/pdf/134.pdf> Doi: 10.3850/978-981-18-2016-8_134-cd
10. Breckpot, M. 2013. *Flood control of river system with Model Predictive Control; the River Demer as a case study*. PhD Thesis, KU Leuven, Belgium.
11. Breckpot, M., Agudelo, O. M., De Moor, B. 2013. Flood control with Model Predictive Control for river systems with water reservoirs. *J. Irrigation and Drainage Engineering* **139**, 532–541.
12. Chaubey, I. Ward, G.M. 2006: Hydrologic budget analysis of a small natural wetland in Southeast USA. *J. Environmental Informatics* **8(1)**, 10–21.
13. Le Coent, P. et al. 2021: Is-it worth investing in NBS aiming at reducing water risks? Insights from the economic assessment of three European case studies. *Nature-based Solutions* , in press. <https://doi.org/10.1016/j.nbsj.2021.100002>
14. Coles, S. 2001: An introduction to statistical modeling of extreme values. Springer series in statistics. pp. 223
15. Environment Agency Leeds 2014-2017. River Aire at Armley, rating change report August 2016. River Aire at Kildwick, flow derivation review November 2015; River Calder at Mytholmroyd, flow derivation review July 2017; River Don at Sheffield Hadfields, flow derivation review November 2014.
16. Environment Agency 2016: Hydrology of the December 2015 Flood in Yorkshire. April 2016 Report of Environment Agency. <https://www.ceh.ac.uk/sites/default/files/2015-2016%20Winter%20Floods%20report%20Low%20Res.pdf> (last access 19 Jun 2021).
17. European Commission 2014: Guide to Cost-Benefit Analysis of Investment Projects: Fletcher, T.D., Shuster, W., Hunt, W.F., Ashley, R., Butler, D., Arthur, S., Trowsdale, S., Barraud,

¹ <https://github.com/obokhove/wetropolis20162020/blob/master/PlansApperleyBridgefloodeasingUpdate.pdf>

- S., Semadeni-Davies, A., Bertrand-Krajewski, J.L., Mikkelsen, P.S., Rivard, G., Uhl, M., Dagenais, D., Viklander, M., 2015. SUDS, LID, BMPs, WSUD and more – The evolution and application of terminology surrounding urban drainage. *Urban Water Journal* **12**, 525–542.
18. B. Hankin, I. Hewitt, G. Sander, F. Danieli, G. Formetta, A. Kamilova, A. Kretzschmar, K. Kiradjiev, C. Wong, S. Pegler, and R. Lamb 2020: A risk-based, network analysis of distributed in-stream leaky barriers for flood risk management. *Hydrology and Earth System Sciences HESS* **20**, 2567–2584.
 19. Hodgkins, G.A., Whitfield, P.H., Burn, D.H., Hannaford, J., Renard, B., Stahl, K., Fleig, A.K., Madsen, H., Mediero, L., Korhonen, J., Murphy, C., Wilson, D. 2017. Climate-driven variability in the occurrence of major floods across North America and Europe. *J. Hydrology* **552**, 704–717.
 20. Huband, M., Palao, E., Heasley, E., Gasca-Tucker, D., Ruggles-Brise 2019: DIY NFM – simple tools for assessing effectiveness of Natural Flood Management. Presentation at Flood and Coast 2019, Telford, UK, <https://www.floodandcoast.com/assets/SpeakerPresentations/2-Hiband.pdf>.
 21. Kelmans, M., Bokhove, O., Kent, T., Hicks, T. Flood mitigation: from outreach demonstrator to a graphical cost-effectiveness diagnostic for policy makers. Submitted Research Excellence Framework Impact Case Study (UK). To be published publicly online in 2021–2022.
 22. Kent, T., Bokhove, O. 2020: Ensuring ‘well-balanced’ shallow water flows via a discontinuous Galerkin finite element method: issues at lowest order. <https://arxiv.org/abs/2006.03370>
 23. Kent, T. 2020: Wetropolis rainfall and flood demonstrator: developments in hydraulic modelling and visualisation. https://github.com/tkent198/hydraulic_wetro
 24. Kent, T., Bokhove, O. 2020–2021: Wetropolis rainfall and flood demonstrator: developments in hydraulic modelling and visualisation. GitHub site: https://github.com/tkent198/hydraulic_wetro.
 25. Kundzewics, Z.W., Hegger, D.L.T., Matczak, P., Driessen, P.P.J. 2018: Flood risk reduction: structural measures and diverse strategies. *Proc. Natl. Acad. Sci. USA* **115**, 12321–12325.
 26. Larsen, A., Larsen, J., Lane, S.N. 2020: Dam busy: beavers and their influence on the structure and function of river corridor hydrology, geomorphology, biogeochemistry and ecosystems. Subm. *Earth Science Reviews*.
 27. Lowe, J.A. et al. 2018: UK Climate Projections 2018 Overview report. <https://www.metoffice.gov.uk/pub/data/weather/uk/ukcp18/sciencereports/UKCP18-Overviewreport.pdf> (last access: 27 June 2021).
 28. Met Office, Official blog of the Met Office news team 28-12-2015: Record breaking December rainfall. <https://blog.metoffice.gov.uk/2015/12/28/record-breaking-december-rainfall/>
 29. Milne A.A. 1928: *The House of Pooh Corner*. Chapter VI. In which Pooh invents a new game and Eeyore joins in. <http://www.lib.ru/MILN/pooh2.txt>
 30. Mott MacDonald 2020: Leeds Flood Alleviation Scheme Phase 2. Step 2 Fluvial Hydraulic Modelling Report. August 2020. https://consult.environment-agency.gov.uk/psc/leeds-city-council-33706/supporting_documents/Fluvial%20Hydraulic%20Modelling%20Report.pdf
 31. Moulopoulou, E.-E. 2018: Understanding gravel beach formation: Tracking waves and wave-bed dynamics through experiments and simulations. PhD dissertation University of Leeds. https://etheses.whiterose.ac.uk/23692/1/Moulopoulou_EE_Mathematics_PhD_2018.pdf
 32. Mueller, D.S., Wagner, C. R. 2009: Measuring discharge with Acoustic Doppler Current Profilers from a moving boat. US Geological Survey. https://pubs.usgs.gov/tm/3a22/pdf/tm3a22_lowres.pdf and <https://pubs.usgs.gov/tm/3a22/>
 33. Muste, M, Lee, K 2013: Quantification of hysteretic behavior in streamflow rating curves. 35th IAHR World Congress, Chengdu, China. doi: 10.13140/2.1.1302.3369
 34. Naiman, R.J., Johnston, C.A., Kelley, J.C. 1988: Alteration of North American streams by beaver. *Bioscience* **38**, 753–762.
 35. Nyssen, J., Pontzele, J., Billi, P. 2020: Effect of beaver dams on the hydrology of small mountain streams: Example from the Chevral in the Ourthe Orientale basin, Ardennes, Belgium. *J. Hydrology* **402**, 92–102.
 36. Pengal, P. et al. 2021: Glinščica for all: exploring the potential of NBS in Slovenia: barriers and opportunities. Chapter 16 in **to do**.

37. Perks, M. 2019: Non-Contact Monitoring—Why Use a Non-Contact Monitoring Approach? <https://flood-obs.com/non-contact-monitoring/> (Latest access 1 July 2020).
38. Perosa, F., Gelhaus, M., Zwirglmaier, V., Airas-Rodriguez, L.F., Zingraff-Hamed, A., Cyffka, B., Disse, M. 2021: Integrated valuation of Nature-Based Solutions using TESSA: three floodplain restoration studies in the Danube Catchment, *Sustainability* **13**, 1482.
39. Piton, G., A. Pagano, R. Basile, B. Cokan, S. Les-jak 2018: DEL6.2 From hazards to risk: models for the DEMOs –Part 5: Slovenia –Glinščicacatchment DEMO. Technical report, NAIAD H2020project. GA no. 730497. http://naiad2020.eu/wp-content/uploads/2019/02/D6.2_REV_FINAL.pdf
40. Puttock, A., Graham, H.A., Cunliff, A.M., Elliott, M., Brazier, R.E. 2017: Eurasian beaver activity increases water storage, attenuates flow and migrates diffuse pollution from intensively-managed grasslands. *Science of the Total Environment* **576**, 430–443.
41. Rahmasary, A.N. 2013: Analisa Hidrologi Bendung Katulampa: Potensi Pengembangannya Sebagai Bendungan Pengendali Banjir Jakarta (Indonesia). Institute Pertanian Bogor. Available at: <https://adoc.pub/analisis-hidrologi-bendung-katulampa-potensi-pengembangannya.html>
42. Ribic, C.A., Donner, D.M., Beck, A.J., Rugg, D.J., Reinecke, S., Eklund, D. 2017: Beaver colony density trends on the Chequamegon-Nicolet national forest, 1987–2013. *PLOS One*, 0170099.
43. Sanderson, M. 2010: Changes in the frequency of extreme rainfall events for selected towns and cities, Met Office “Ofwat” report. https://www.ofwat.gov.uk/wp-content/uploads/2015/11/rpt_com_met_rainfall.pdf (last access: 29 June 2021).
44. Septianus, N. 2020: Can we improve flood protection? M.Sc. thesis in Data Science, University of Leeds, Leeds, UK. <https://github.com/Flood-Excess-Volume/RiverCiliwung/blob/main/DissertationfinalNicoSeptianus.pdf>
45. Sheffield City Council 2017: Protecting Sheffield from flooding. Upper Don and Sheaf catchments. Natural Flood Management workshop. Presentation Arup & Sheffield City Council.
46. Stocker, T. F., Qin, D., Plattner, G.-K., Tignor, M., Allen, S. K., Boschung, J., Nauels, A., Xia, Y., Bex, V., and Midgley, P. M. (Eds.) 2013: IPCC 2013: Summary for Policymakers, in: Climate Change 2013: The Physical Science Basis. Contribution of Working Group I to the Fifth Assessment Report of the Intergovernmental Panel on Climate Change, Cambridge University Press, Cambridge, UK, New York, NY, USA.
47. Vermuyten E., Meert P., Wolfs V., Willems P. 2018. Combining model predictive control with a reduced genetic algorithm for real-time flood control. *J. Water Resources Planning and Management* **144**, in press. doi:10.1061/(ASCE)WR.1943-5452.0000859
48. Woo, M.-K., Waddington J.M. 1990: Effects of beaver dams on subarctic wetland hydrology. *Arctic* **43**, 223–230.
49. West Yorkshire Combined Authority 2016: Leeds City Region Flood Review Report—December 2016. Available online: <https://www.the-lep.com/media/2276/leeds-city-region-flood-review-report-final.pdf> (last access: 29 June 2021).
50. Van Alphen, S. 2019: Room for the River: Innovation, or Tradition? The Case of the Noordwaard. In: *Adaptive Strategies for Water Heritage*. pp 308–323.